Technical Report
Project NS033

NATIONAL INSTITUTE FOR FOREST PRODUCTS INNOVATION

Development and implementation of forest health and biosecurity systems and protocols based on quantitative pest risk and economic impact assessment

Calibrated pest spread models for the broader GT with which to quantitatively investigate the invasion ecology and economic impacts of forestry pests

2025

Mount Gambier Centre
Funded by the Australian Government, South Australian Government & Industry Partners.
nifpi.org.au

Development and implementation of forest health and biosecurity systems and protocols based on quantitative pest risk and economic impact assessment

Calibrated pest spread models for the broader GT with which to quantitatively investigate the invasion ecology and economic impacts of forestry pests

Prepared for

National Institute for Forest Products Innovation

Mount Gambier

by

D. Smith and R. Hoffman, D. Patzel and J. O'Hehir

Publication: Development and implementation of forest health and biosecurity systems and protocols based on quantitative pest risk and economic impact assessment - Calibrated pest spread models for the broader GT with which to quantitatively investigate the invasion ecology and economic impacts of forestry pests

Project No: NIF082-1819 Part A [NS033]

IMPORTANT NOTICE

ISBN: 978-1-922718-66-2

Researcher/s:

Anna Weeks, John Weiss, Kathryn Sheffield and David Smith
Agriculture Victoria,
Department of Jobs, Precincts and Regions

D. Patzel and J. O'Hehir
STEM, University of South Australia

This work is supported by funding provided to Forest and Wood Products Australia (FWPA) to administer the **National Institute for Forest Products Innovation** program by the Australian Government Department of Agriculture, Fisheries and Forestry and the Government of South Australia in partnership with the University of South Australia.

Australian Government
Department of Agriculture, Fisheries and Forestry

Government of South Australia
Department of Primary Industries and Regions

Innovative Forest Health and Biosecurity for the Green Triangle

Technical manual

Anna Weeks, John Weiss, Kathryn Sheffield and David Smith

Agriculture Victoria, Department of Jobs Precincts and Regions.

April, 2021

Acknowledgments

The modelling presented in this overview is based on the 3PG+ forest growth model is described in Feikema *et al*. (2010). Source code has been adapted from the CAT1D and 3PG+ code written by Dr Craig Beverly, Agriculture Victoria (Beverly, C., 2009).

Authors would like to acknowledge The National Institute for Forest Products Innovation and The University of South Australia.

About

This report has been created as using Live Code File Format (.mlx), MATLAB (2021). Results presented in this report are linked directly to the currently modelled scenario and may change with different species parameter sets. Modelled outcomes are based on a representative forestry estate and are not intended to provide an exact representation of specific sites and/or management procedures. The 'kml' folder attached to this report contains spatialised views of the regions and modelled outputs that can be viewed in Google Earth Pro (https://www.google.com/earth/versions/#download-pro).

Version

Version: V1.0.1

Table of Contents

Introduction

The "Innovative Forest Health and Biosecurity for the Green Triangle" project was developed to create a Green-Triangle focussed, integrated, forest health and biosecurity system (including response scenarios) utilising pest spread forecasts and economic impacts to plantation (profitability, control costs and loss of markets). The modelling component of this work looks to link the established agent-based pest dispersal model (Weiss *et al*., 2019) to the 3PG+ Forest Growth Model Feikema *et al*. (2010) to provide better insights into the impact of pest incursion on forestry production. Key outputs from the 3PG+ Forest Growth model, used to populate the economic model, include

- Stand stocking rate, modified by mortality, thinning and tree removal for pest incursion management
- Biomass $(\mathrm{kg/tree}), (\mathrm{kg/ha})$ partitioned into branch, stem, foliage, litter and root
- Carbon $(\mathrm{kg}\ C/\mathrm{ha})$ partitioned into branch, stem, foliage, litter, root and soil carbon
- Stand volume (m^3/ha) with and without branch
- Stand litter (m^3/ha)
- Diameter at breast height (m)
- Root depth (mm), Root projection area (m^2) and Crown projection area (m^2)
- Tree height (m)
- Mean annual increment $(m^3/\mathrm{ha}/\mathrm{year})$

Overview and Development

The original 3PG forest growth model was developed by Landsberg and Waring (1997) as a process-based, stand-level model where photosythetically active radiation absorbed by the forest canopy $(\mathrm{APAR}\ (\mathrm{MJ}/m^2/\mathrm{month}))$ is modified by a series of environmental factors then multiplied by a canopy quantum efficiency factor $(\alpha_c\,(g\,C/\mathrm{MJ}))$ to estimate net primary production $(g\,C/m^2/\mathrm{month})$. The 3PG+ model (Feikema *et al*. (2010)) provided further enhancements including the spatial attribution of soils, climate and topographical data to parameterise the fully distributed water balance model of the Catchment Analysis Tool (CAT) (Beverly *et al*., 2005; Weeks *et al*., 2011). This provided a more dynamic representation of available water in the root zone and enhanced representation of the environmental modifiers. Additional modifications included an early-stage radiation interception function, mortality functions, salinity and drought responses.

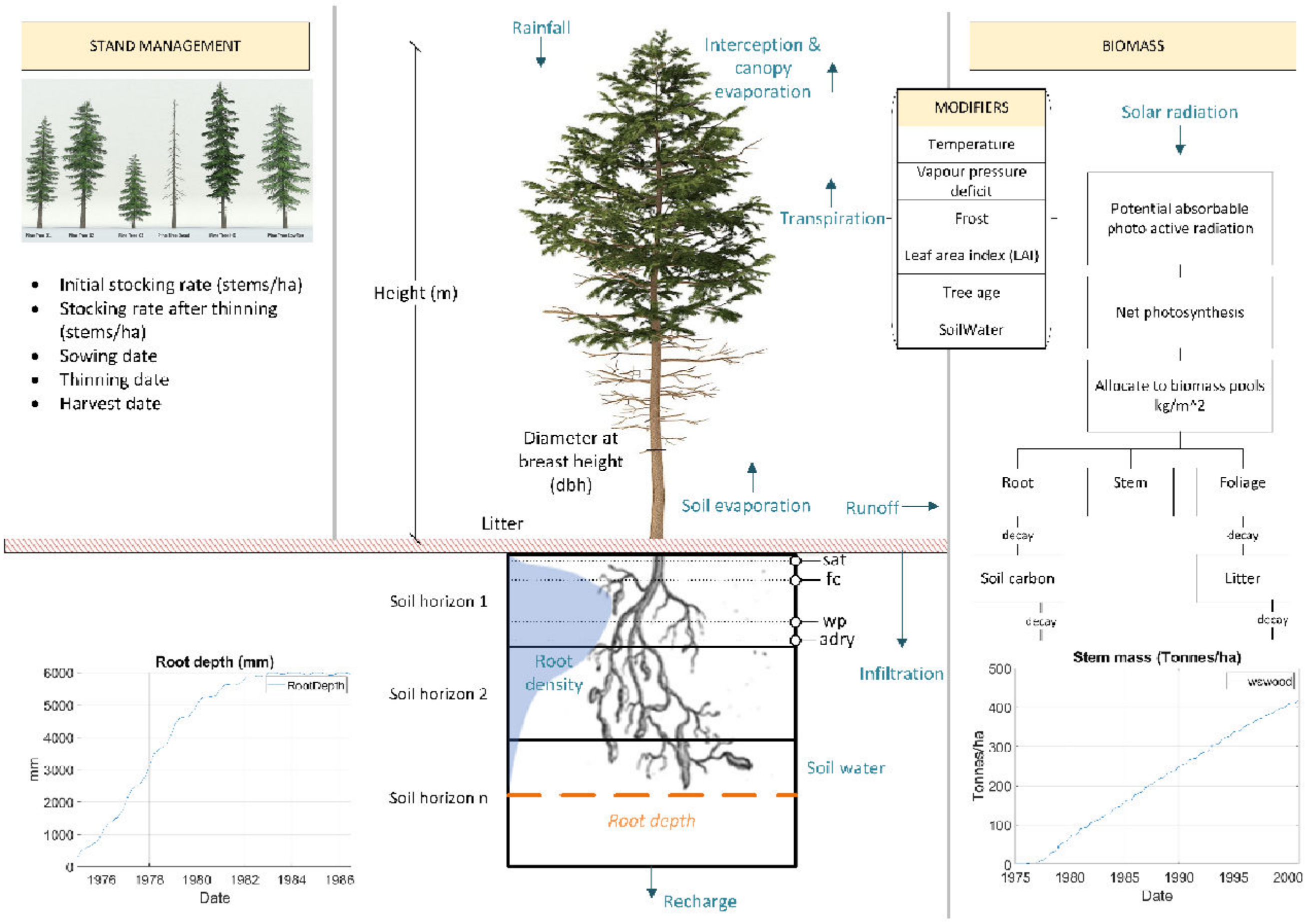

Figure 1. 3PG+ forest growth model

In response to the requirements of modelling pest outbreaks a small number of further modifications have been made to the model outlined in Feikema *et al*. (2010). The original 3PG+ module ran on a monthly time step, consistent with Landsberg and Waring (1997). On a functional level, the module has now been modified to run on a daily time step to bring it in line with the daily water balance calculations of the Catchment Analysis Tool (CAT) and pest dispersal functions.

Tree age, health and water stress can be strong factors in the establishment and spread of pest species. Significant pest incursions can lead to tree mortality in effect creating a scenario of dynamic stocking rates within a stand. Pest mitigation responses such as thinning, and tree removal also modify stand stocking rates and subsequent light and water resources available to the tree. To better account for the changing light and water resources available to individual trees within a stand under dynamic stocking rates the following modifications were made.

- Crown projection area $(\mathrm{CPA}\ (m^2/\mathrm{tree}))$ was estimated as a function of diameter at breast height (DBH) using the Power-sigmoid functional model described in Shimano, (1997). The maximum crown projection area of an individual tree was limited by the stocking density $\left(\mathrm{CPA}_{\mathrm{max}} = 10000\, m^2/(n\ \ \mathrm{trees/ha})\right)$, occurring at full canopy closure of the stand. Net primary production was then calculated for the individual tree $(g\, C/\mathrm{tree/month})$ from the photosythetically active radiation available to the tree $(\mathrm{APAR}_{\mathrm{tree}} = \mathrm{APAR.\,CPA}\ (\mathrm{MJ/tree/month}))$. This approach saw subdued tree growth rates at higher stocking densities due to the limited radiation interception once canopy closure has occurred. Assuming a uniform stand of trees, stand dynamics were calculated by multiplying tree growth responses by the stocking rate. As this approach described the incomplete canopy coverage for young stands of trees it also effectively replaced the early-stage radiation interception function that was introduced into 3PG+.
- Root projection area $(\mathrm{RPA}\ (m^2/\mathrm{tree}))$ was estimated using a similar approach however was not limited by stocking density. Instead, when total root cover exceeded the stand area an element of competition was created. Potential transpiration $\mathrm{PoT}\ (\mathrm{mm})$ was calculated using the Penman Monteith approach (Allen *et al*. (1998)) as a function of the tree leaf area index. The potential transpiration was then modified to account for competition from over-stocked stands $\mathrm{PoTmod} = \mathrm{PoT.}\dfrac{n.\,\mathrm{RPA}}{10000}\ (\mathrm{mm})$. Actual transpiration was still limited by available soil water. A transpiration stress factor was then calculated as the ratio of actual to potential transpiration where $1 = \text{no stress}, 0 = \text{maximum stress}$. This approach saw increased transpiration stress with a lack of soil water which was further enhanced by higher stocking densities as total root projection area exceeded the stand area. Transpiration stress was also used to drive the mortality function which was previously described in 3PG+ by the -3/2 power self-thinning law and did not account for environmental factors.

Catchment Analysis Tool (CAT) water balance model

The water balance model is based on the Catchment Analysis Tool CAT1D model (Beverly, et al., 2005; Weeks et al., 2008), a biophysical model that simulates the plant-soil-water dynamics for agricultural systems. The model runs on a daily time-step with climate inputs including daily rainfall, potential evapotranspiration (PET), vapour pressure deficit, minimum and maximum temperature and solar radiation sourced from the SILO 0.05° gridded Data Drill Jeffrey et al., 2001 (https://www.longpaddock.qld.gov.au/silo/datadrill/). Topographical inputs are derived from the Geoscience Australia (https://ecat.ga.gov.au/geonetwork/srv/eng/catalog.search#/metadata/69888) hydrologically corrected 30m digital elevation model and include slope, aspect, drainage basins and flow accumulation. The dominant soil type was sourced from the Australian Soil Resource Information System (ASRIS) http://www.asris.csiro.au/themes/Atlas.html and described using a Northcote(1972) classification, attributed using the 50th percentile predictions of soil properties described in McKenzie et. al (2000). Soils are characterised by the number and soil profiles, the volumetric water content (mm) of each profile at air-dry (adry), wilting point (wp), field capacity (fc) and saturation (sat), and the saturated hydraulic conductivity, $\mathrm{ksat}\ (\mathrm{mm/day})$, of the soil profiles.

Rainfall interception at the canopy level is calculated as a funtion of Leaf Area Index (LAI). Intercepted water is held in the canopy and contributes to total evapotranspiration of the stand, limited by Potential Evapotranspiration (PET). Rainfall that penetrates the canopy and reaches the forest floor either infiltrates the soil profile or runs off the surface as excess. The partitioning of rainfall into infiltration and runoff is calculated as a function of rainfall, litter-cover, slope and saturated hydraulic conductivity. Water is redistributed through the soil profile based on a linear cascading bucket model where the capacity of each bucket is the equivalent of the saturated water content of each soil horizon. Soil evaporation occurs from the top two soil profiles and is based on Ritchie's two-stage evaporation algorithm (Ritchie, 1972). After infiltration, $\mathrm{Stage}\ I$ drying occurs to a specified limit at a potential rate which is calculated as a function of cover and potential evaporation. $\mathrm{Stage\ II}$ drying then continues to occur up to the limit due to diffusive evaporative processes that are related to the slope of the drying curve and the number of days since rain.

Potential transpiration (mm) for an individual tree with root projection area $(\mathrm{RPA}\ (m^2))$ is estimated using the Penman Monteith calculation. Vertical root density, described by the function DFAC specifies the percentage of the potential transpiration to be extracted from each soil profile. Actual transpiration is limited by available water within the soil profile. After transpiration is accounted for, excess water above field capacity is transferred to the lower soil profile at a rate limited by the saturated hydraulic conductivity of the layer. Any further excess water above saturated capacity is assigned to lateral subsurface flows . Soil water is updated at each time-step to account for gains from infiltration and irrigation and losses through soil evaporation, transpiration, lateral flow, and infiltration to the lower soil profile. In the final step , irrigation, transpiration, soil evaporation and soil water are summed over all soil profiles, recharge is estimated as the water transferred through the lowest soil profile and lateral flows are summed and combined with the runoff term.

3PG+ Model parameterisation and review

The following is an analysis of the 3PG+ model at a select number of points in the landscape. The analysis provides an overview of the underlying algorithms that support the 3PG+ model.

	Polygon	DEM (m)	Slope (deg)	Aspect (degN)	Soil depth (m)	Datadrill climate statio
No thinning	1	65	0	90	6	{'140.80_37.95'}
1 thinning	2	65	0	90	6	{'140.80_37.95'}
2 thinnings	3	65	0	90	6	{'140.80_37.95'}
3 thinnings	4	65	0	90	6	{'140.80_37.95'}

3PG+ Model overview

Species parameter sets are presented in Appendix C.

Biomass production and allocation

Radiation interception

The net photosynthetically active radiation $(\phi_{\text{net}}\,(\text{MJ}/m^2))$ is estimated using the Penman Monteith approach which accounts for net longwave and net shortwave radiation at a specified latitude, longitude and elevation. The photosythetically active radiation (ϕ_p) for an individual tree within a uniform stand is then described as

$$\phi_p = \text{CPA}.\,\phi_{\text{net}}\ (\text{MJ})$$

where CPA is the estimated crown projection area (m).

The amount of ϕ_p that is absorbed (ϕ_{pa}) is calculated by Beer's law

$$\phi_{\text{pa}} = \phi_p\left(1 - e^{(-k_\varphi.\text{LAI}_{\text{tree}})}\right)\ (\text{MJ})$$

where k_φ is the species specific extinction coefficient and LAI_{tree} is the leaf area index (m^2/m^2) for an individual tree within a uniform stand.

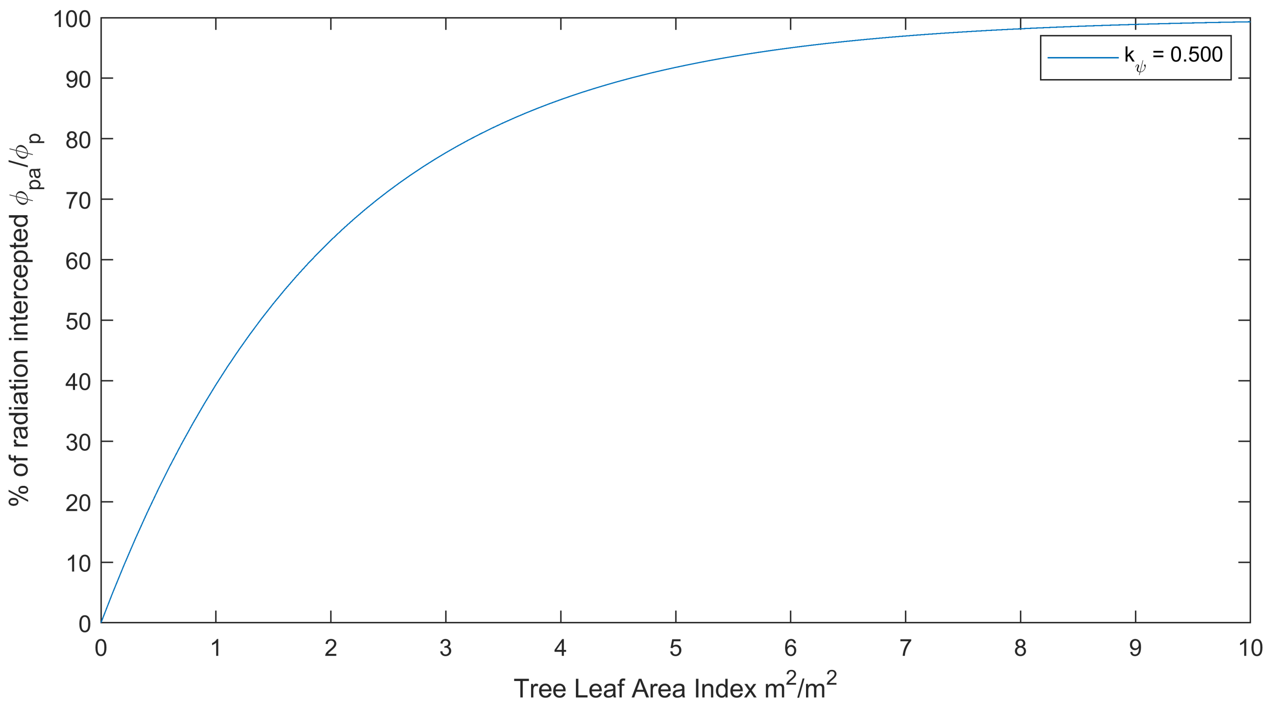

Figure 2. Percent radiation interception (ϕ_{pa}/ϕ_p) as a function of Leaf Area Index

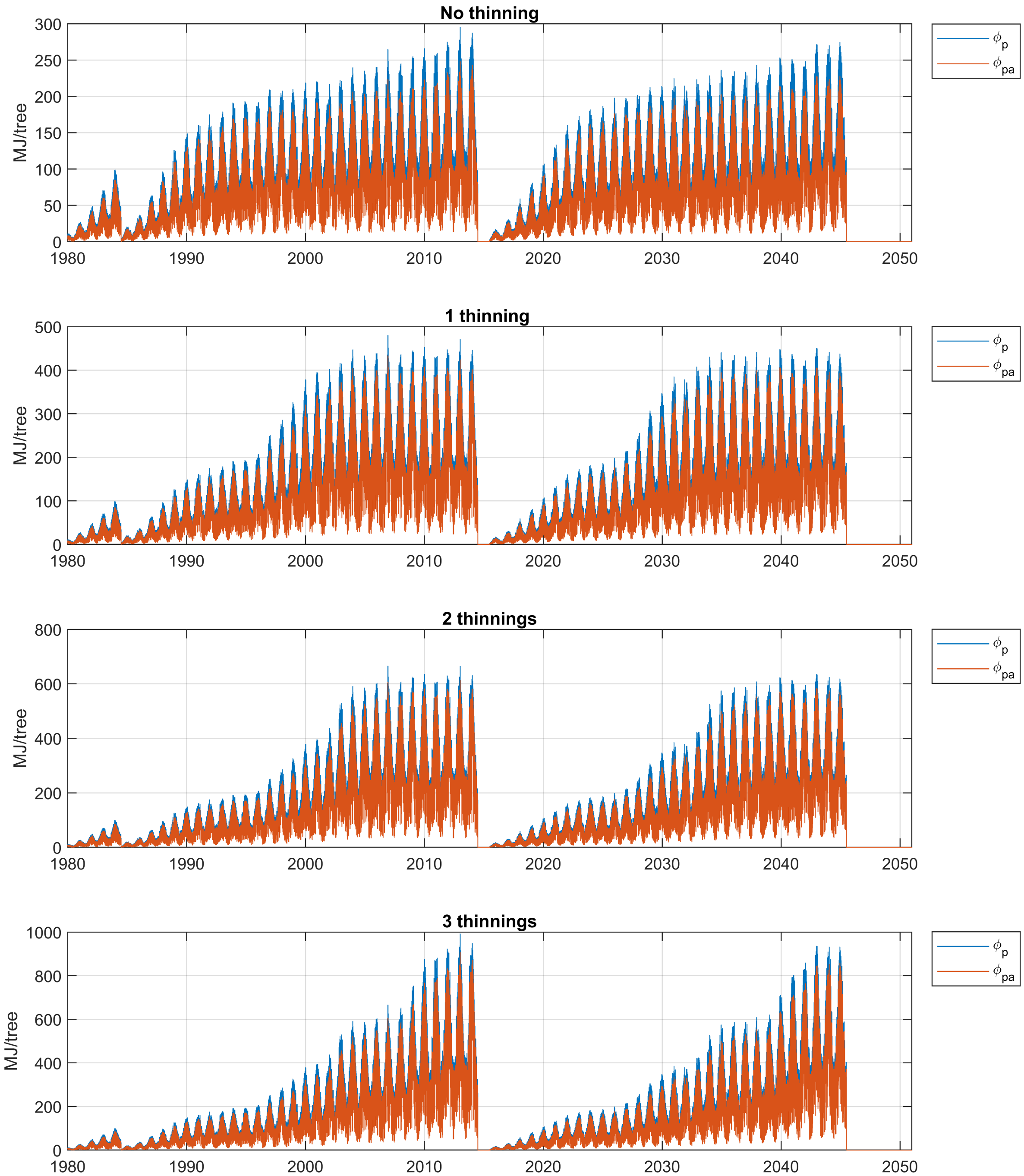

Figure 3. The net (ϕ_p) and absorbed (ϕ_{pa}) photosythetically active radiation for an individual tree within a uniform stand

The utilisable absorbed photosynthetically active radiation (ϕ_{pau}) is calculated as the product of the absorbed photosynthetically active radiation (ϕ_{pa}) and a series of modifiers with values ranging between 0 and 1.

$$\phi_{\mathrm{pau}} = \min(f_\theta, f_{\mathrm{VPD}}) f_{\mathrm{age}} f_{\mathrm{temp}} f_{\mathrm{frost}} \,(\mathrm{MJ/tree})$$

Where f_θ is a function of transpiration deficit; f_{VPD} is the stomatal response to daytime vapour pressure deficit; f_{temp} is the temperature response function; f_{frost} modifies growth when $T_{\mathrm{min}} < 0$ and f_{age} is a function of tree age.

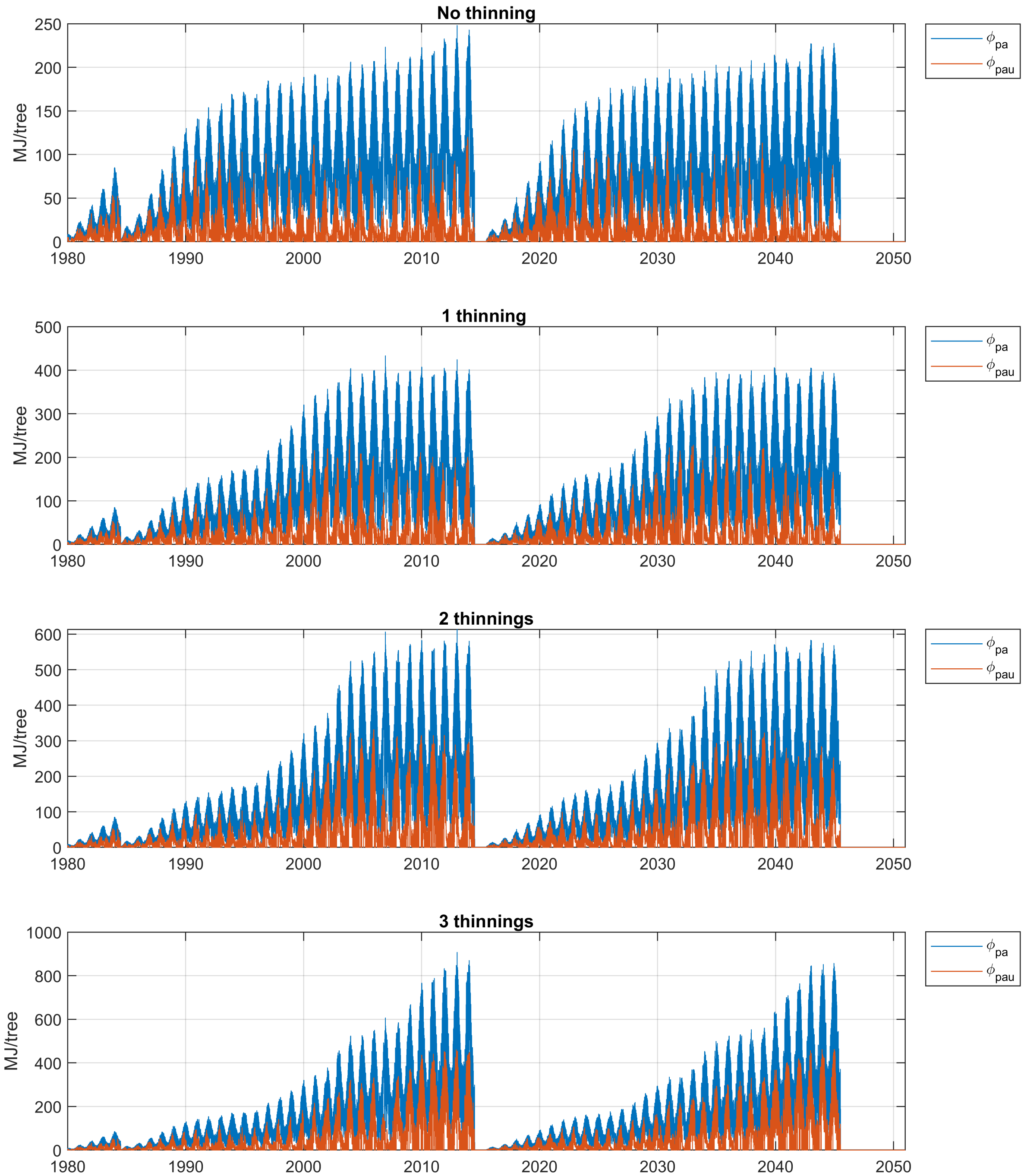

Figure 3. The absorbed (ϕ_{pa}) and utilisable absorbed (ϕ_{pau}) photosythetically active radiation for an individual tree within a uniform stand

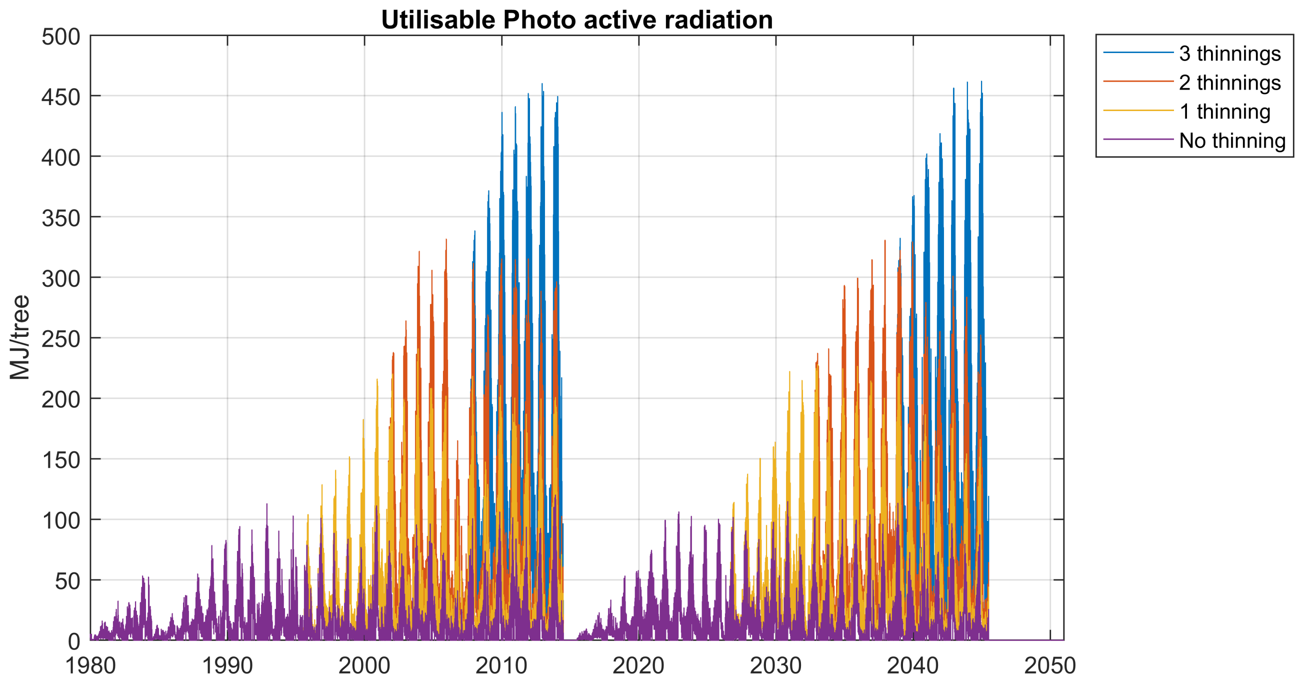

Figure 4. Utilisable Photo active radiation (MJ/tree)

Growth Modifiers

Transpiration deficit modifier

Potential Transpiration of the stand $(\mathrm{PT_{stand}})$ is estimated as the rate of Penman Monteith transpiration for an individual tree $(\mathrm{PT_{tree}}\ (\mathrm{mm}))$ multiplied by the root projection area $(\mathrm{RTA}\ (m^2))$ and stocking rate $(\mathrm{stocking}\ (\mathrm{trees/ha}))$ of the stand. When stand root projection area exceeds the total stand area, within-stand competition occurs, resulting in increased transpiration deficit and an overall reduction in tree growth.

$$\mathrm{PT_{stand}} = \mathrm{PT_{tree}}.\ \mathrm{RTA}.\ \frac{\mathrm{stocking}}{10000}\ (\mathrm{mm})$$

Actual transpiration T_{stand} through the soil profiles is limited by the vertical root density (DFAC) and the plant available soil water (PAW) of the soil profile

$$T_{\mathrm{stand}} = \sum_{i=1}^{N\ \mathrm{soil\ profiles}} \min(\mathrm{PT_{stand}}.\ \mathrm{DFAC}_i, \mathrm{PAW}_i)$$

$$\text{where } \sum_{i=1}^{N\ \mathrm{soil\ profiles}} \mathrm{DFAC} = 1$$

The transpiration deficit modifier (f_θ) is then described as

$$f_{\theta} = \frac{T_{\mathrm{stand}}}{\mathrm{PT}_{\mathrm{stand}}}$$

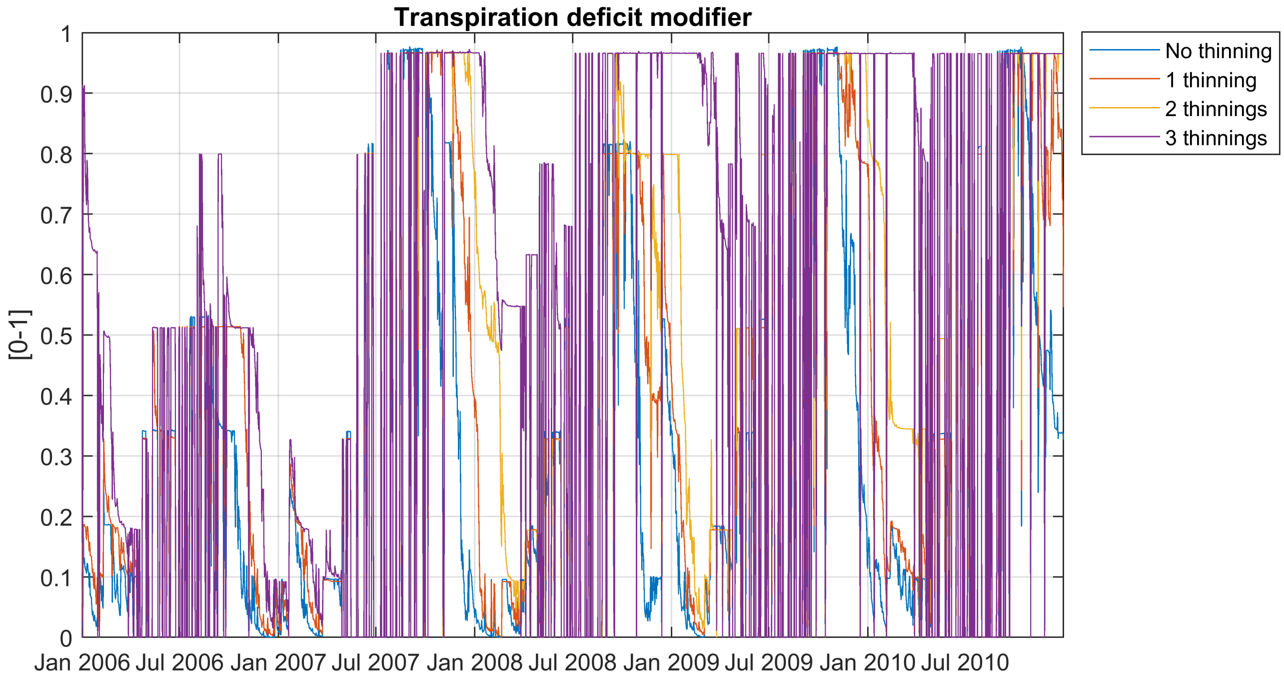

Figure 5. Transpiration deficit modifier ([0-1])

Vapour Pressure Deficit Modifier

The vapour pressure deficit modifier (f_{VPD}) is described by

$$f_{\mathrm{VPD}} = e^{(-k_g \mathrm{VPD})}$$

where k_g is a species-specific parameter based on relationships between conductance and vapour pressure deficit (VPD) (Dye and Olbrich, 1993; Leuning, 1995; Granier *et al.*, 1996)

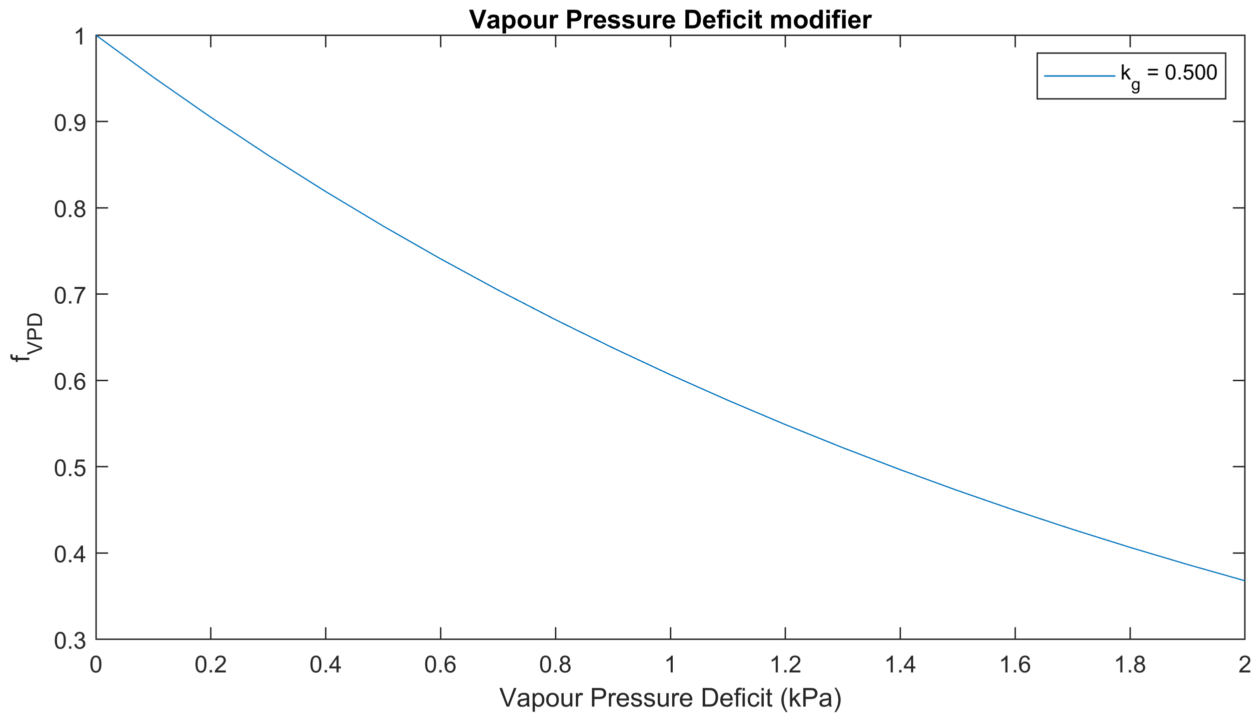

Figure 6. Vapour pressure deficit modifier (f_{VPD}) as a function of VPD

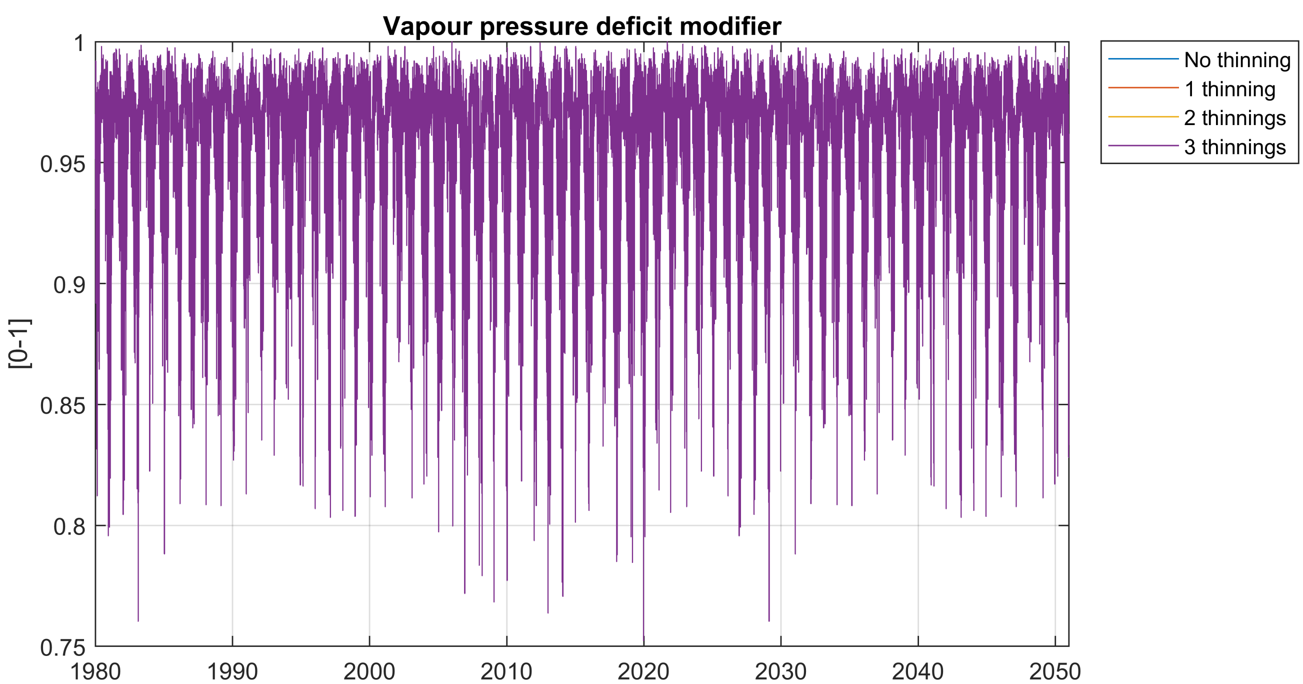

Figure 7. Vapour pressure deficit modifier ([0-1])

Age Modifier

As a forest ages the net primary production decreases. The age modifier (f_{age}) mimics the changes in above-ground wood production shown in data collated by Ryan et. al (1996).

$$f_{\text{age}} = \frac{1}{1 + (\text{age}/0.95.\text{age}_{\text{max}})^{n_{\text{age}}}}$$

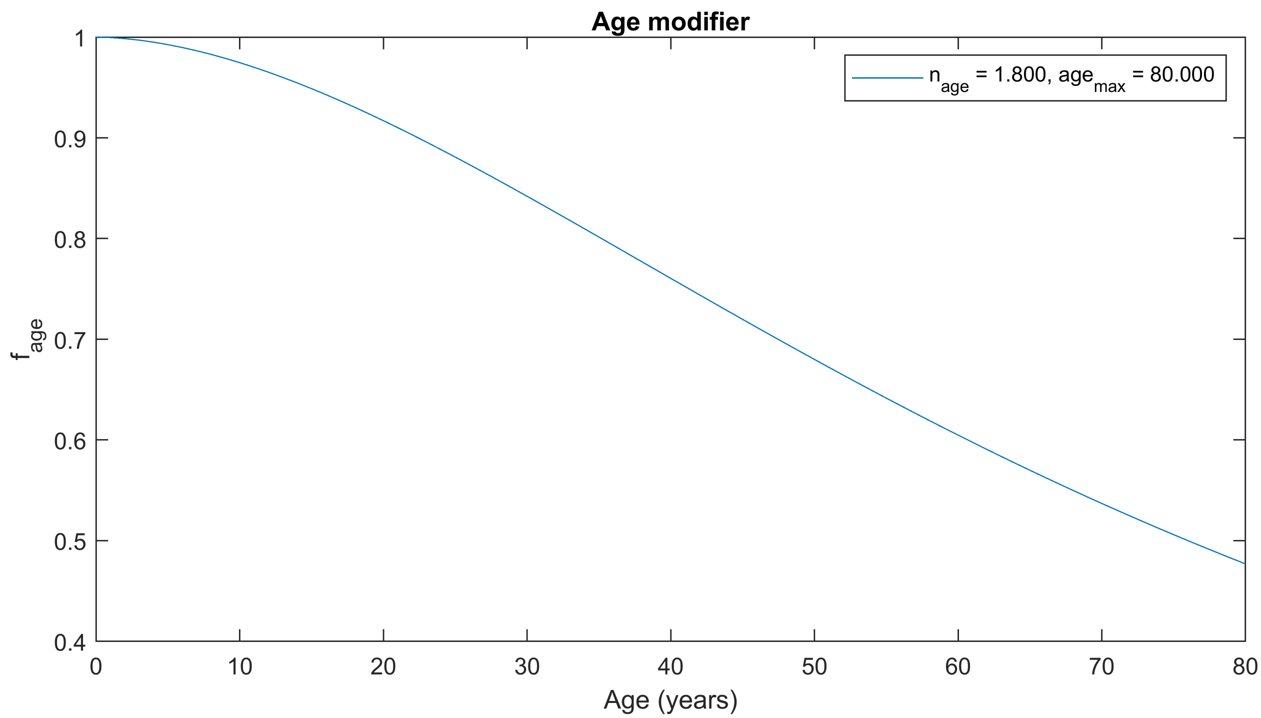

Figure 8. Age modifier (f_{age}) as a function of stand age

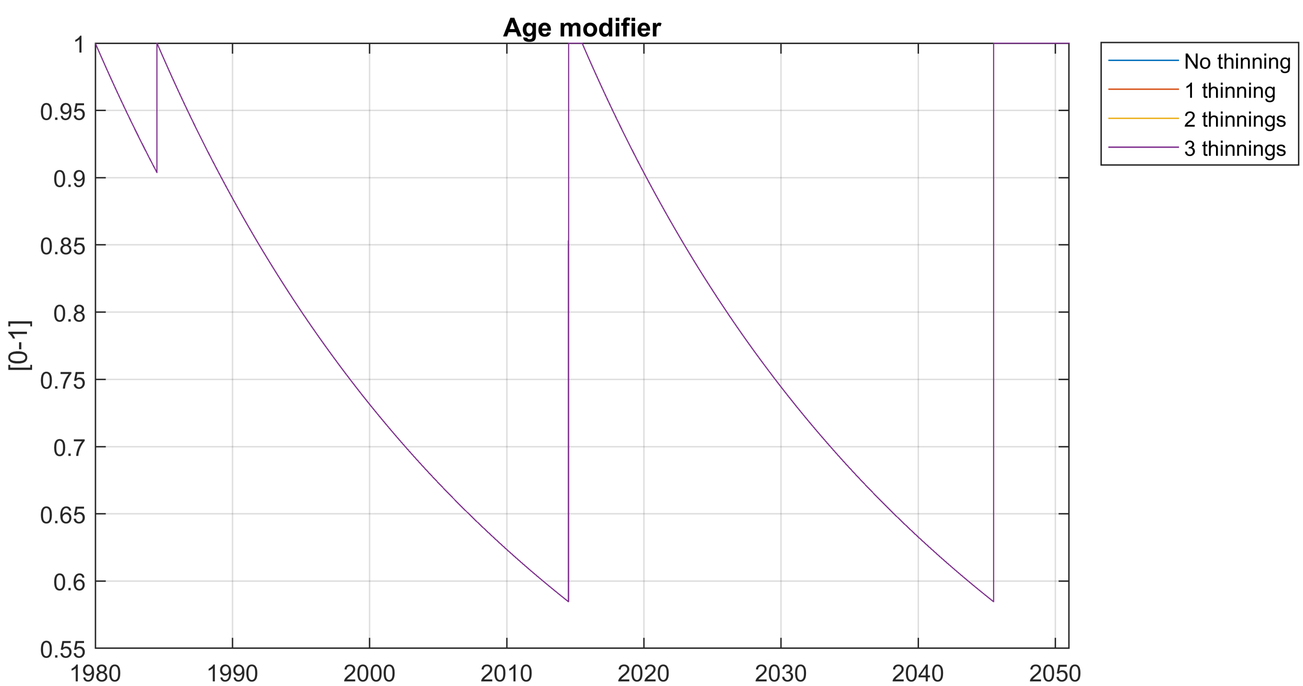

Figure 9. Age modifier ([0-1])

Temperature Modifier

Sands and Landbsberg (2002) introduced an environmental modifier to consider the effects of temperature on growth. The temperature modifier f_T is defined as

$$f_T(T_a) = \left(\frac{T_a - T_{\min}}{T_{\text{opt}} - T_{\min}}\right)\left(\frac{T_{\max} - T_a}{T_{\max} - T_{\text{opt}}}\right)^{(T_{\max}-T_{\text{opt}})/(T_{\text{opt}}-T_{\min})} \text{ where } f_T > 0$$

The parameters $T_{\min}$, T_{opt} and $T_{\max}$ are minimum, optimum and maximum temperatures for net photosynthetic production.

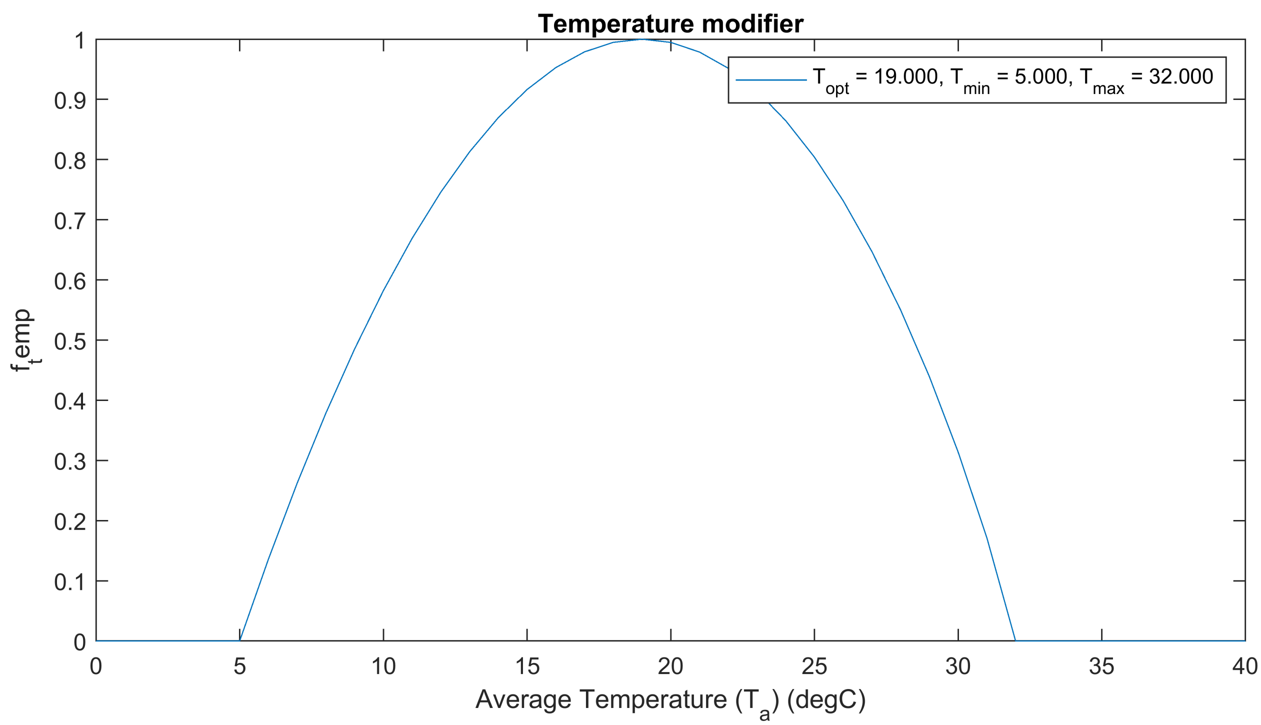

Figure 10. Temperature modifier (f_{temp}) as a function of average temperature

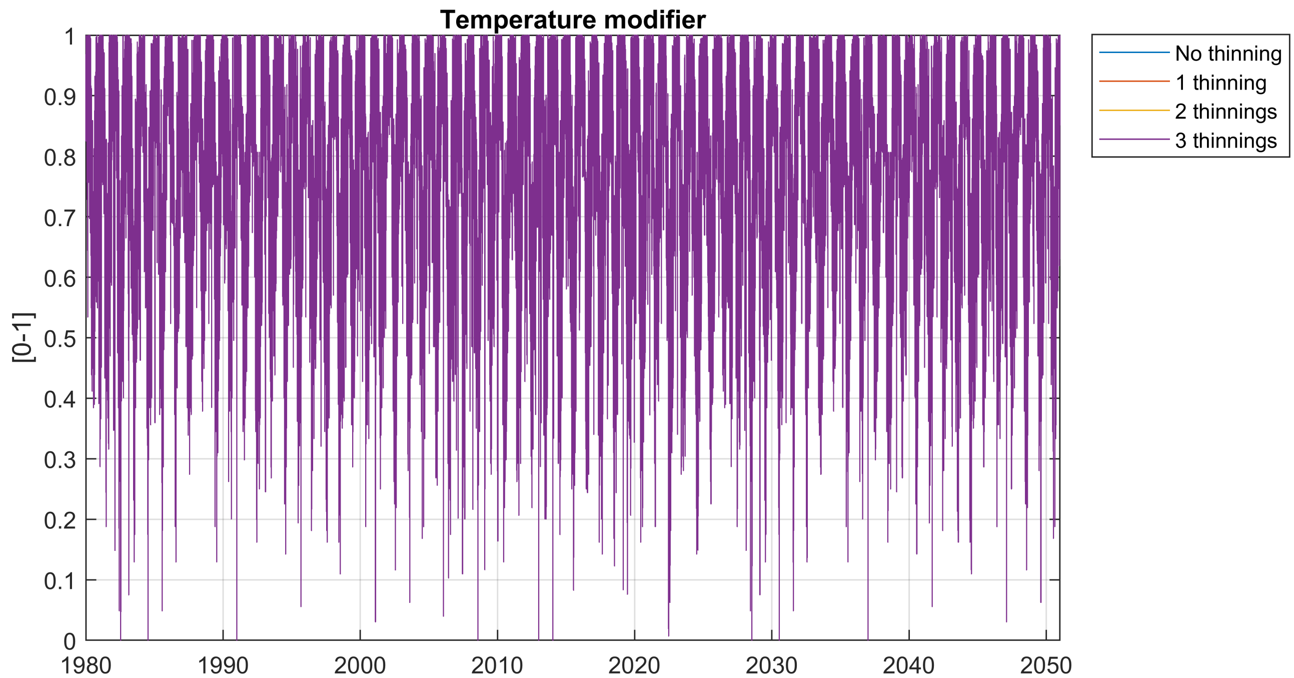

Figure 11. Temperature modifier ([0-1])

Frost Modifier

Frost modifier reduces photosythesis on days where the minimum temperature falls below 0

$$f_{\text{frost}} = \begin{cases} 0.5 & T_{\min} < 0\,\text{degC} \\ 1 & \text{otherwise} \end{cases}$$

Biomass conversion

Gross primary production (GPP) is calculated by multiplying ϕ_{pau} by the canopy quantum efficiency coefficient (α_c) which converts the photosynthetically active radiation from $\text{MJ}\ m^{-2}$ to $g\ C\ m^{-2}$.

$$\text{GPP} = \alpha_c.\phi_{\text{pau}}$$

Net primary production is calculated as

$$\text{NPP} = \text{cpp}.\,\text{GPP}$$

where cpp is a constant fraction (~0.47) of GPP which is assumed to be lost to respiration (Waring *et al.* 1998).

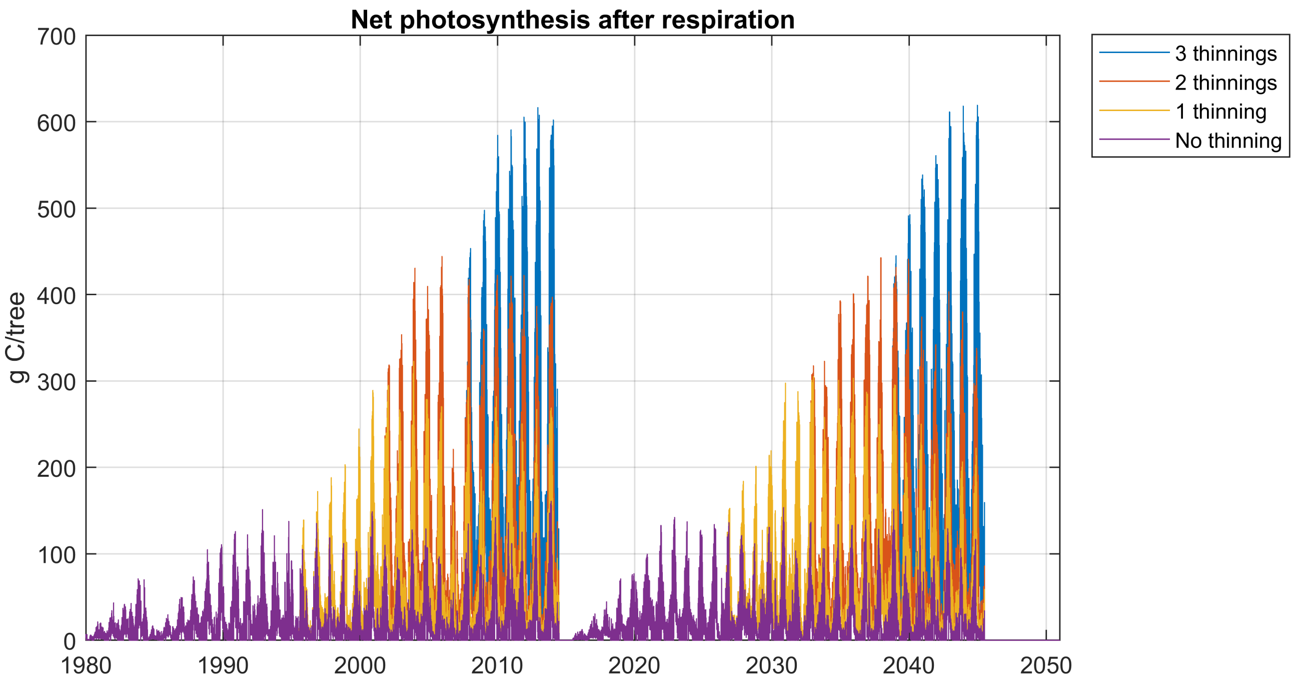

Figure 12. Net Primary Production (NPP) g C/tree

Biomass allocation

Net primary production is allocated to foliage, stem and root pools based on allocation coefficients $\eta_f, \eta_s, \text{and } \eta_r$. As environmental conditions become harsher, the fraction of NPP allocated annually to fine root growth increases from about 25% to nearly 60% (Santantonio, 1989; Runyon *et al*. 1994; Beets and Whitehead, 1996).

Root allocation

The allocation coefficient for roots (η_r) that defines the allocation of NPP to roots is determined by

$$\eta_r = \frac{\text{rootco1}}{1 + \text{rootco2}. \, (\phi_{\text{pau}}/\phi_{\text{pa}})}$$

where the harshness of the environment is defined in terms of the ratio $\frac{\phi_{\text{pau}}}{\phi_{\text{pa}}}$

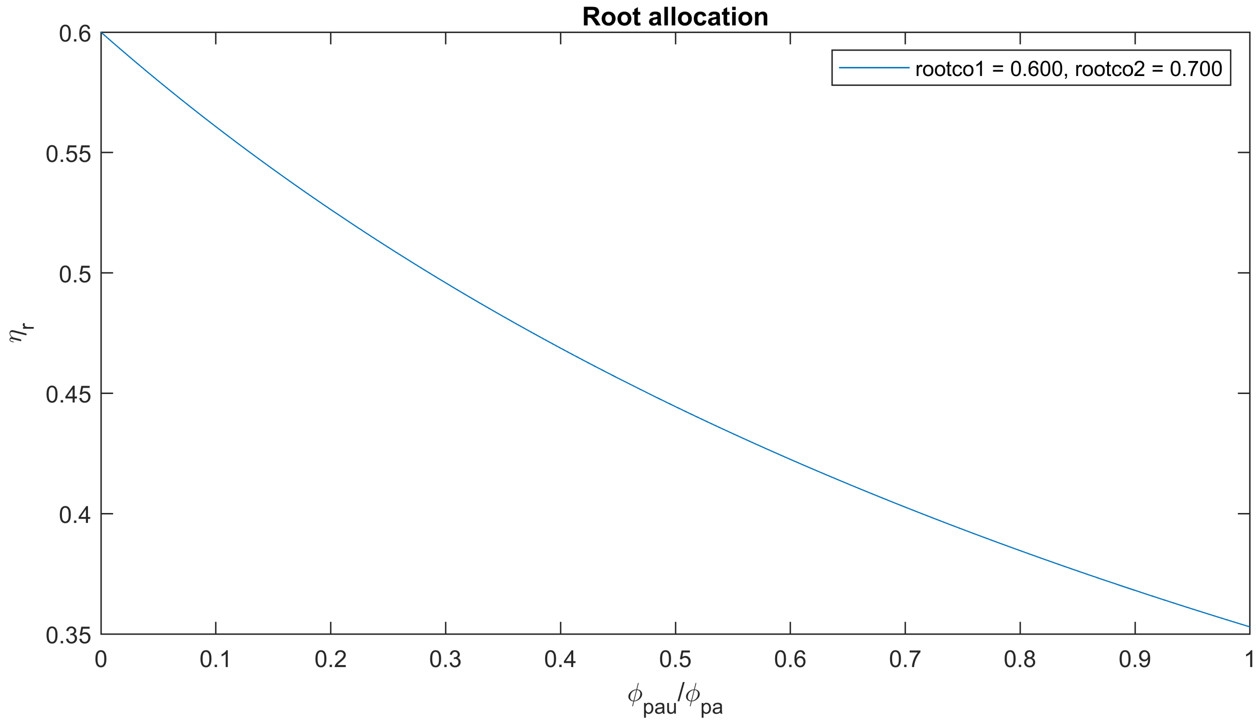

Figure 13. Root allocation (η_r) as a function of environmental stress

Foliage and stem allocation

The above ground stem allocation (η_s) and foliage allocation (η_f) are calculated as

$$\eta_s = \frac{(1-\eta_r)}{(1+p_{f.s})} \text{ and } \eta_f = 1 - \eta_s - \eta_r$$

Where $p_{f.s}$ is the ratio of growth rates of foliage and stems with respect to the tree diameter at breast height (dbh)

$$p_{f.s} = \frac{a_f n_f \text{dbh}^{(n_f - 1)}}{a_s n_s \text{dbh}^{(n_s - 1)}}$$

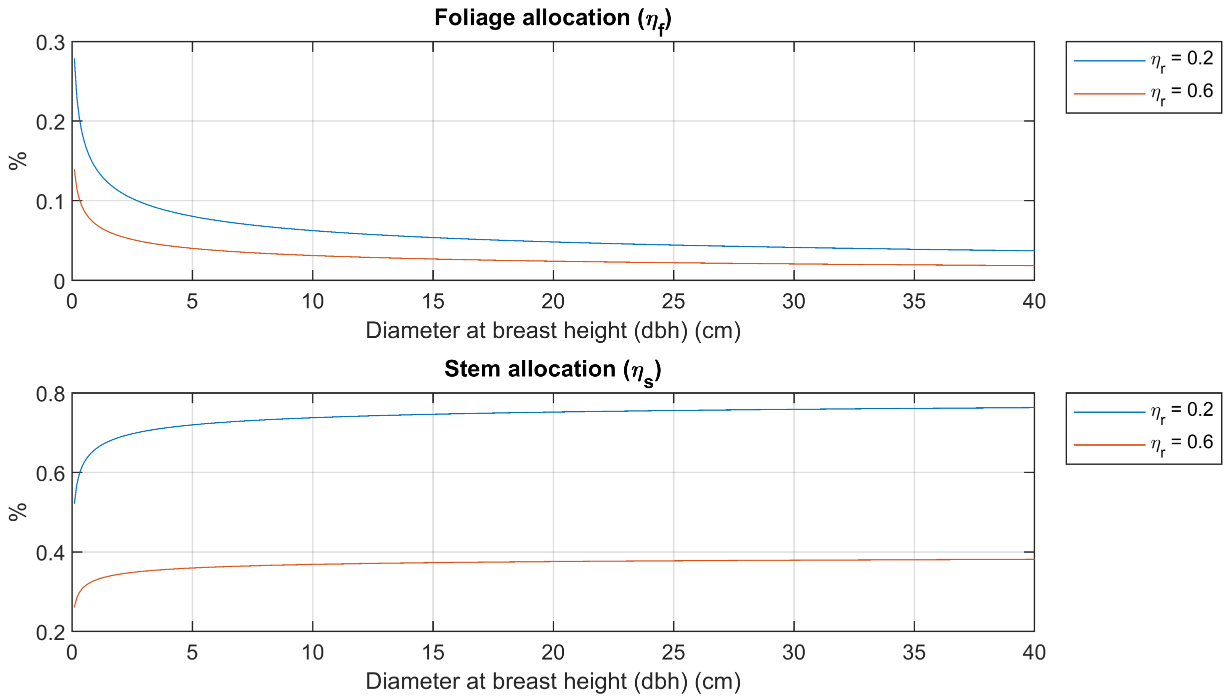

Figure 14. Foliage and stem allocation coefficients as a function of tree diameter at breast height (dbh). a_f = 0.015, n_f = 2.300, a_s = 0.060, n_s = 2.700.

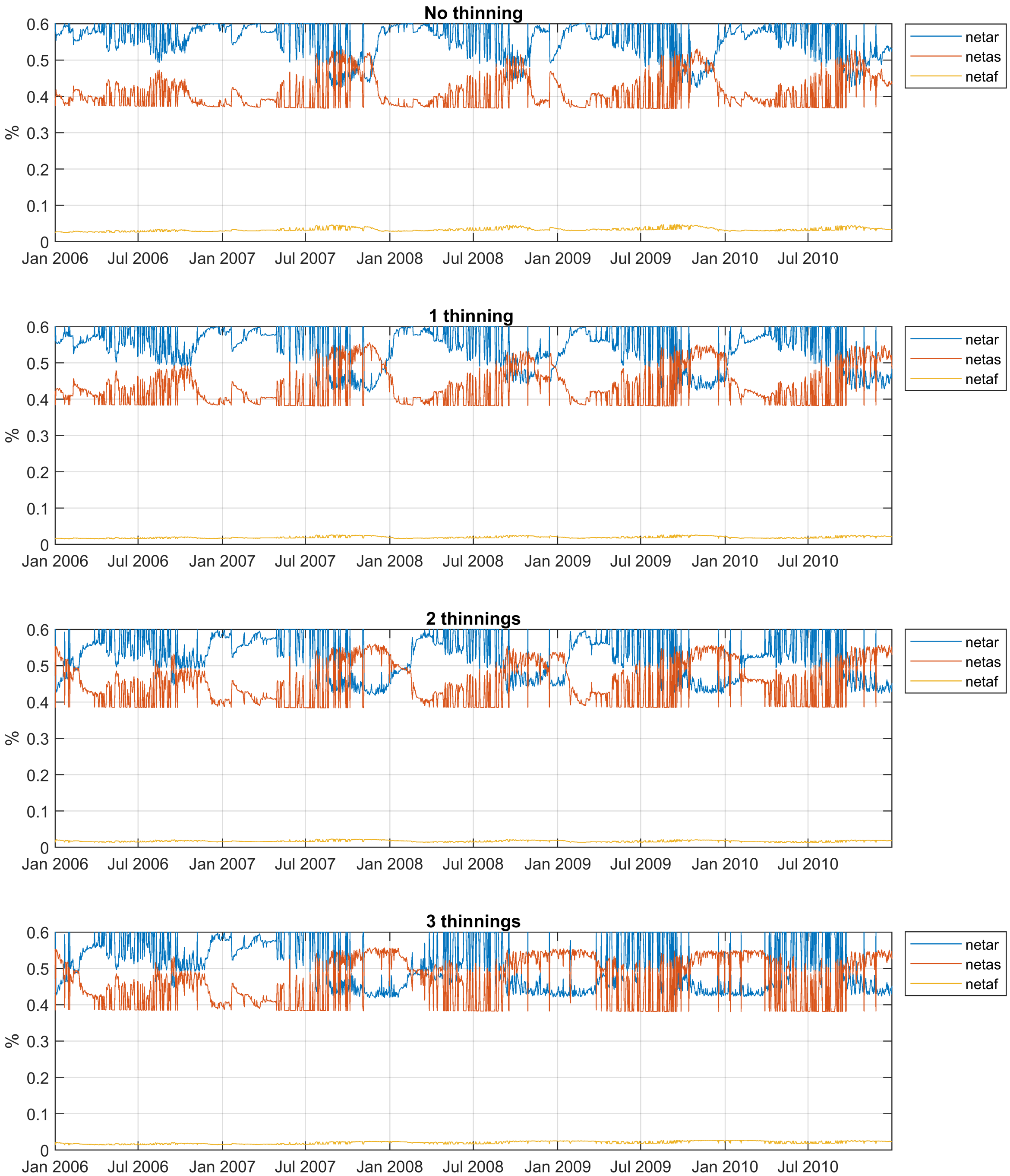

Figure 15. Root, stem and foliage allocaton coefficients

Stem, foliage and root biomass

Stem biomass $(\mathrm{kg\ tree}^{-1})$ at time (t) is calculated as

$$w_s(t) = w_s(t-1) + \eta_s(t)(\mathrm{NPP}(t)).\frac{\mathrm{ctbiomass}}{1000}$$

where the constant $\mathrm{ctbiomass} \approx 2.2\ \mathrm{kg\ drymatter}/\mathrm{kg}\ C$, derived from the assumption that drymatter is approximately 45% carbon.

Foliage biomass $(\mathrm{kg\ tree}^{-1})$ at time (t) is calculated as

$$w_f(t) = w_f(t-1) + \eta_f(t)(\mathrm{NPP}(t)).\frac{\mathrm{ctbiomass}}{1000} - \mathrm{litter}(t)$$

where litter is the daily litterfall biomass.

Root biomass $(\mathrm{kg\ tree}^{-1})$ at time (t) is calculated as

$$w_r(t) = w_r(t-1) + \eta_r(t)(\mathrm{NPP}(t)).\frac{\mathrm{ctbiomass}}{1000} - \delta_{\mathrm{root}}(t)$$

Where $\delta_{\mathrm{root}}(t)$ is the root decay to soil carbon at time t.

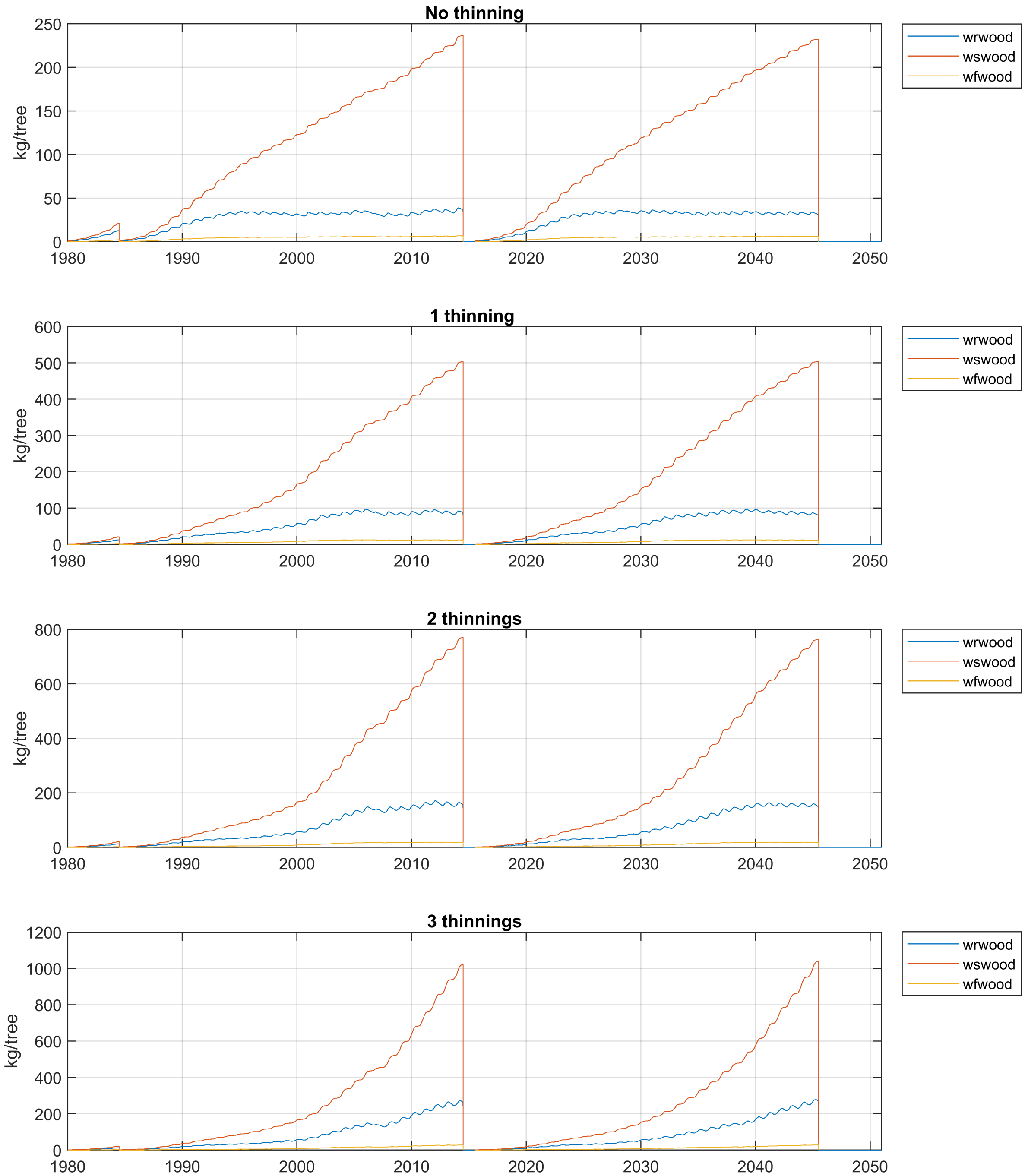

Figure 16. Root, stem and folliage biomass (kg/tree)

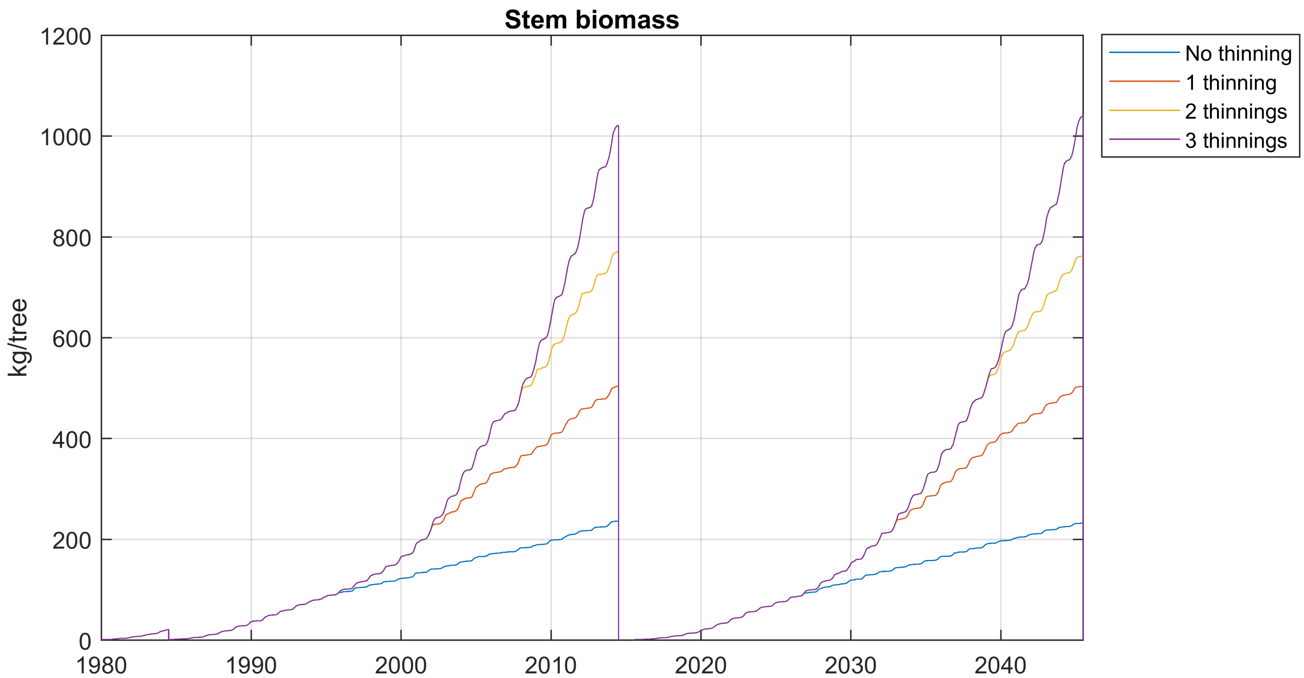

Figure 17. Stem biomass (kg/tree)

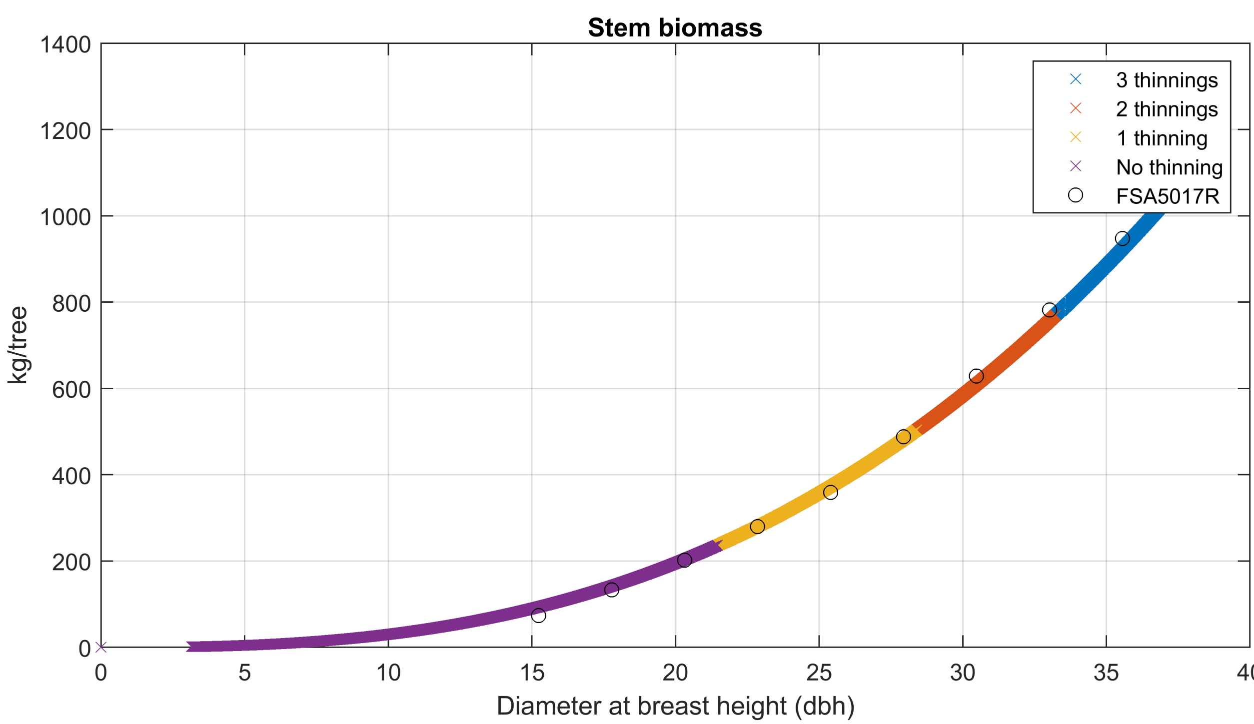

Figure 18. Stem biomass as a function of diameter at breast height (dbh). Validated against FSA5017R: Weight of lobolly pines vs. diameter at breast height, https://www.uaex.edu/publications/pdf/fsa-5017.pdf

Litterfall

The rate of litterfall tends to be in the order of 25% of foliage production per year. Landsberg and Waring (1997) calculated litterfall as a proportion of foliage mass and age with litter rates near zero at year one, reaching a maximum by about 5 years.

The base litter rate (γ_f) is approximated by a Weibull cumulative distribution function

$$\gamma_f = \gamma_{\max}\mathrm{wblcdf}\left(\mathrm{age}, c_\gamma, k_\gamma\right) = \gamma_{\max}.\left(1 - \exp\left(-\left(\mathrm{age}/c_\gamma\right)^{k_\gamma}\right)\right)$$

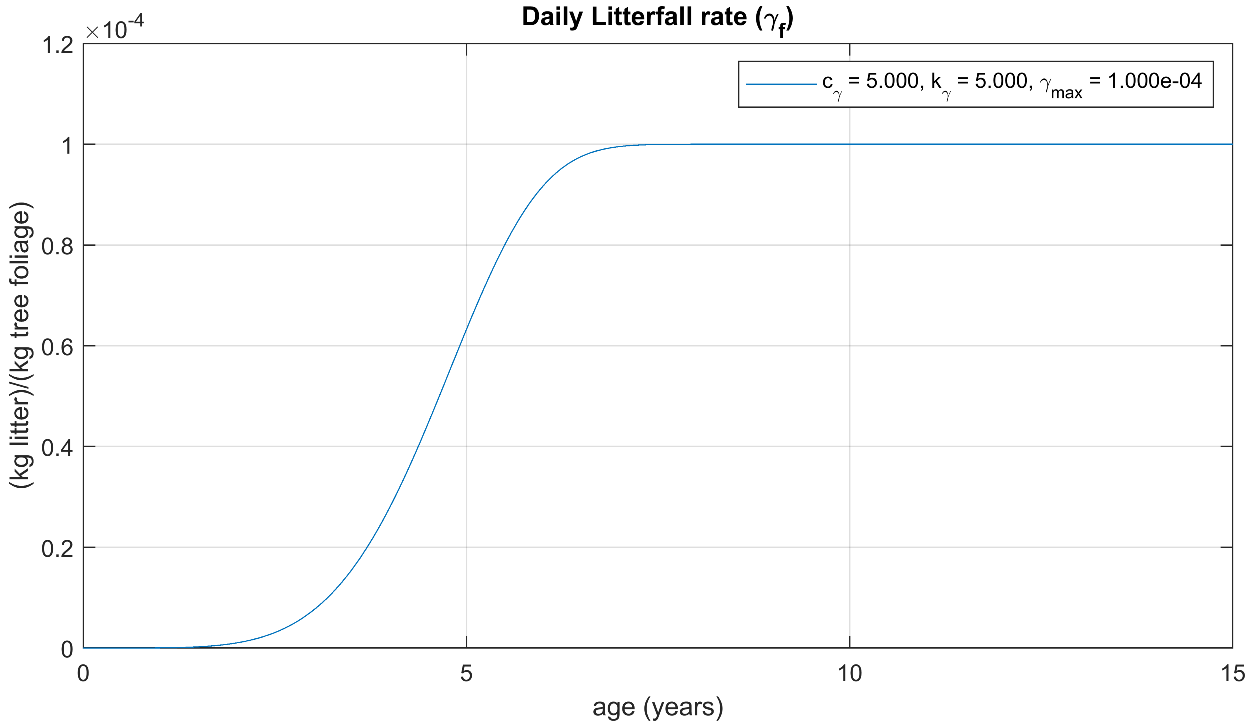

Figure 19. Daily rate of litterfall (γ_f) (kg litter/kg tree foliage)

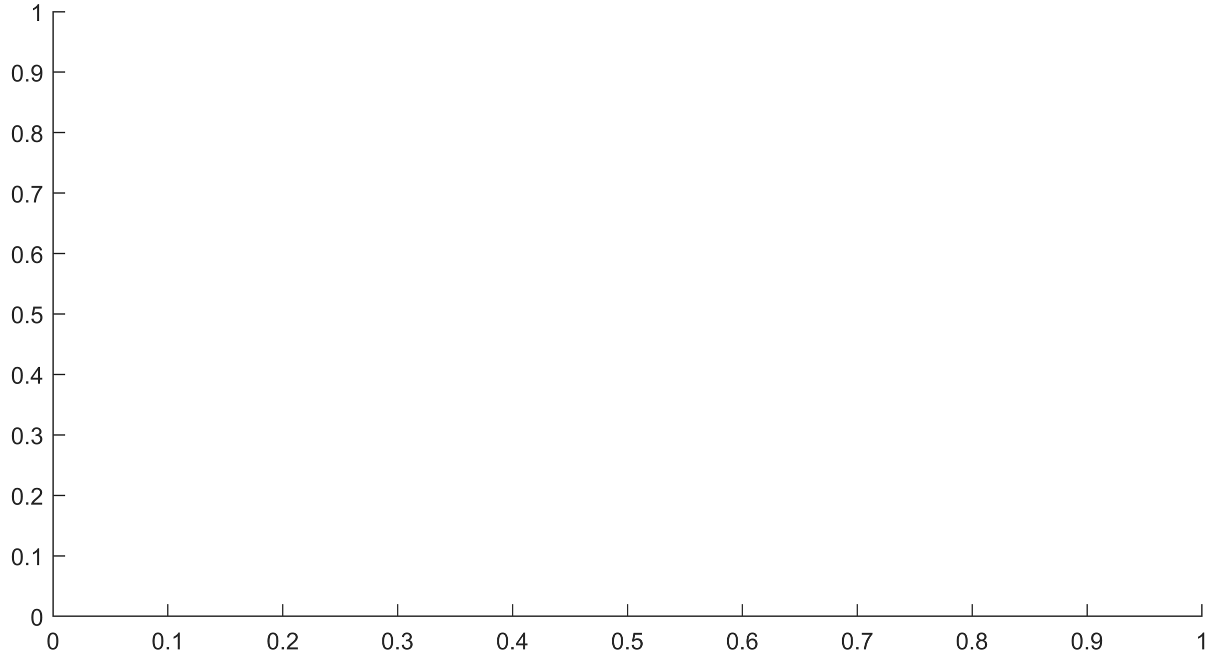

Enhanced litterfall due to drought

When the transpiration deficit modifier f_θ falls below a critical species-specific threshold (l_{thresh}), then the litterfall is enhanced;

$$\gamma_f = \gamma_f + (n.\gamma_{\max} - \gamma_f)\frac{l_{\text{thresh}} - f_\theta}{l_{\text{thresh}}}$$

Stocking rates

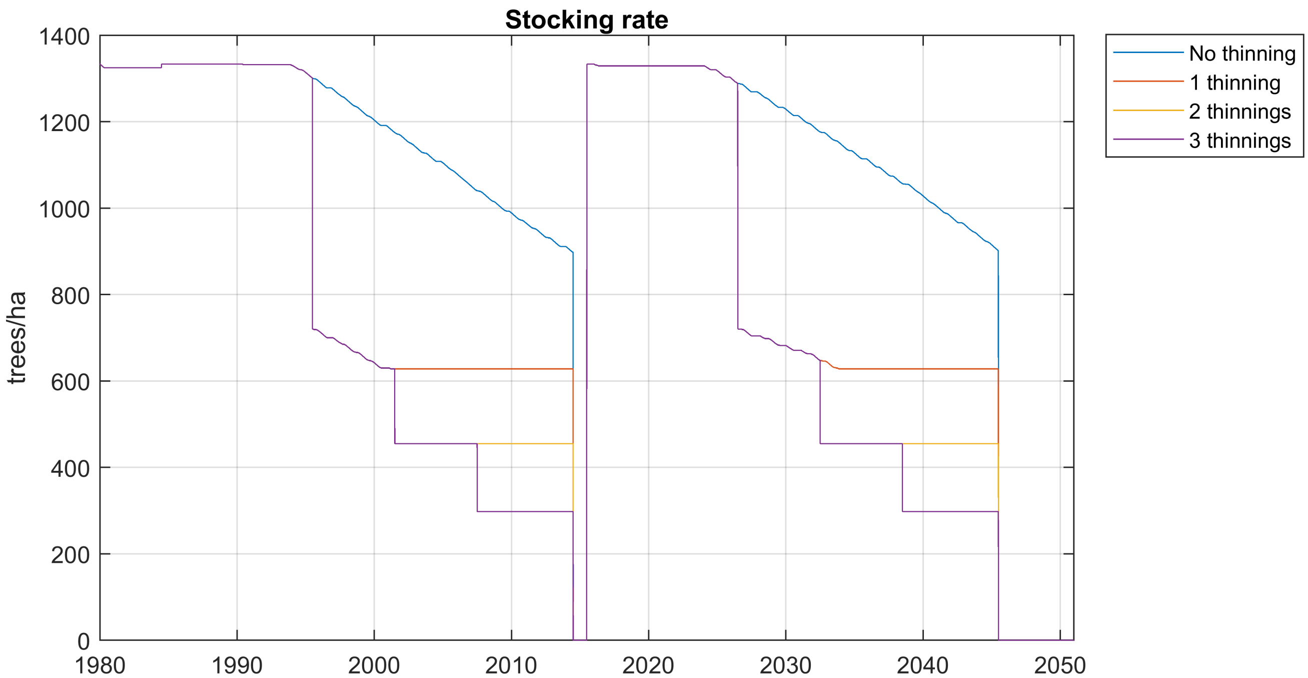

Figure 20. Stocking rate (trees/ha)

Leaf Area Index (LAI)

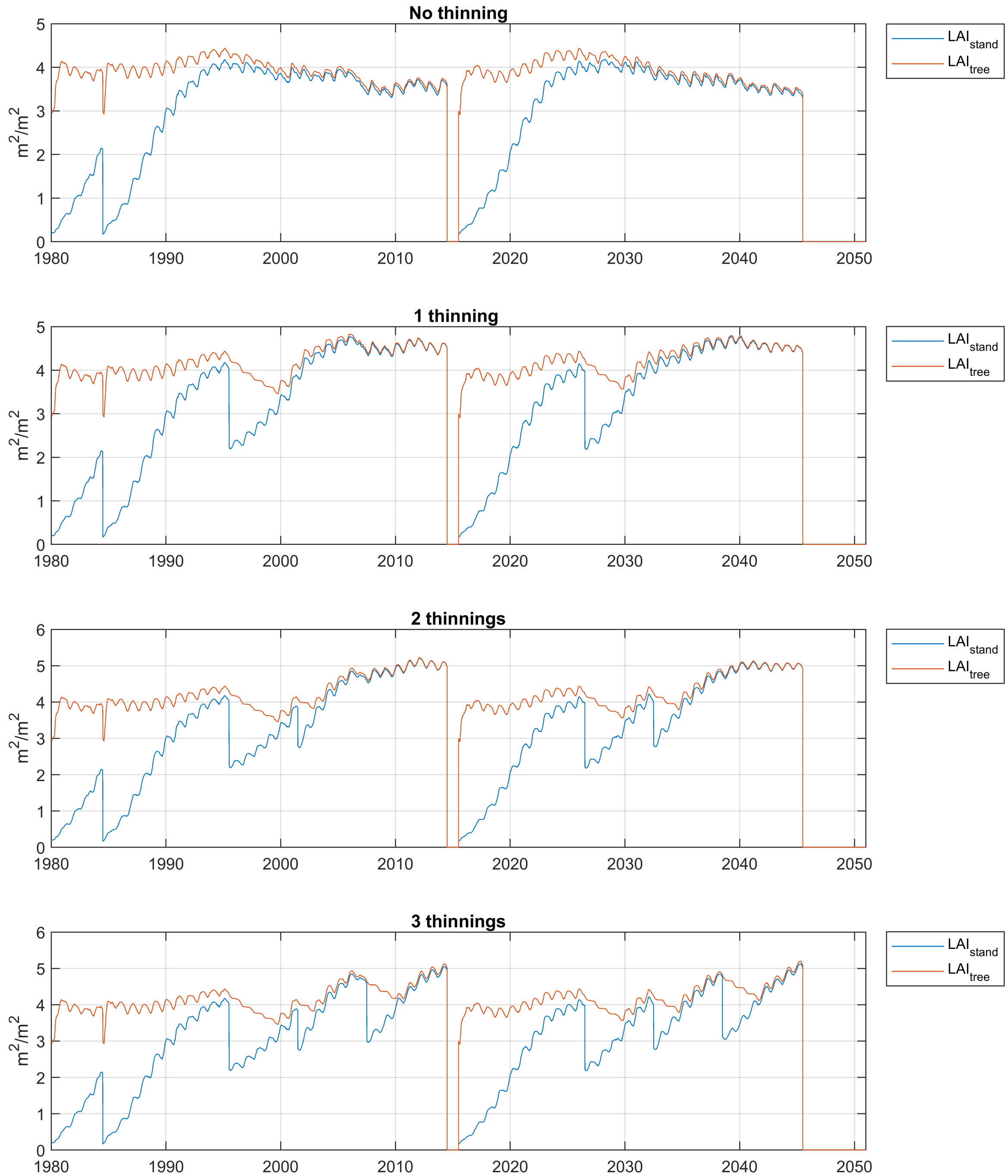

Figure 21. The Leaf Area Index of the stand (LAI_{stand}) approaches the Leaf Area Index of the tree (LAI_{tree}) with canopy closure

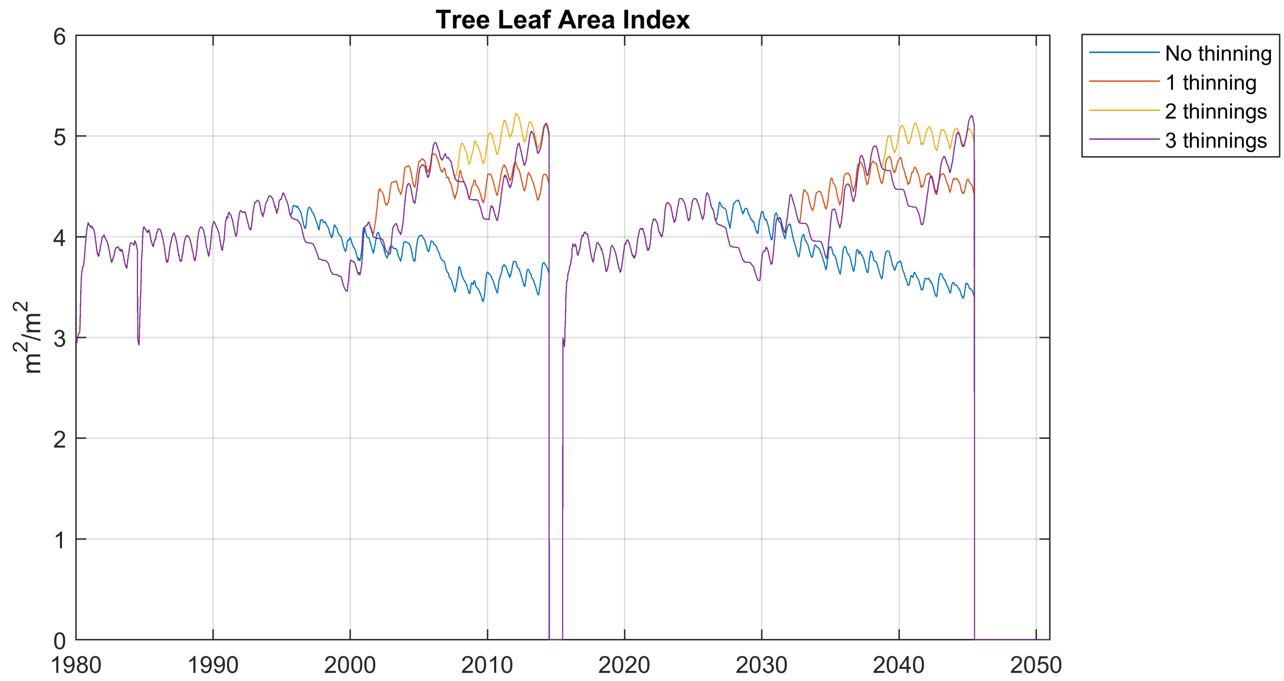

Figure 22. Tree Leaf Area Index (m^2/m^2)

Stand volume

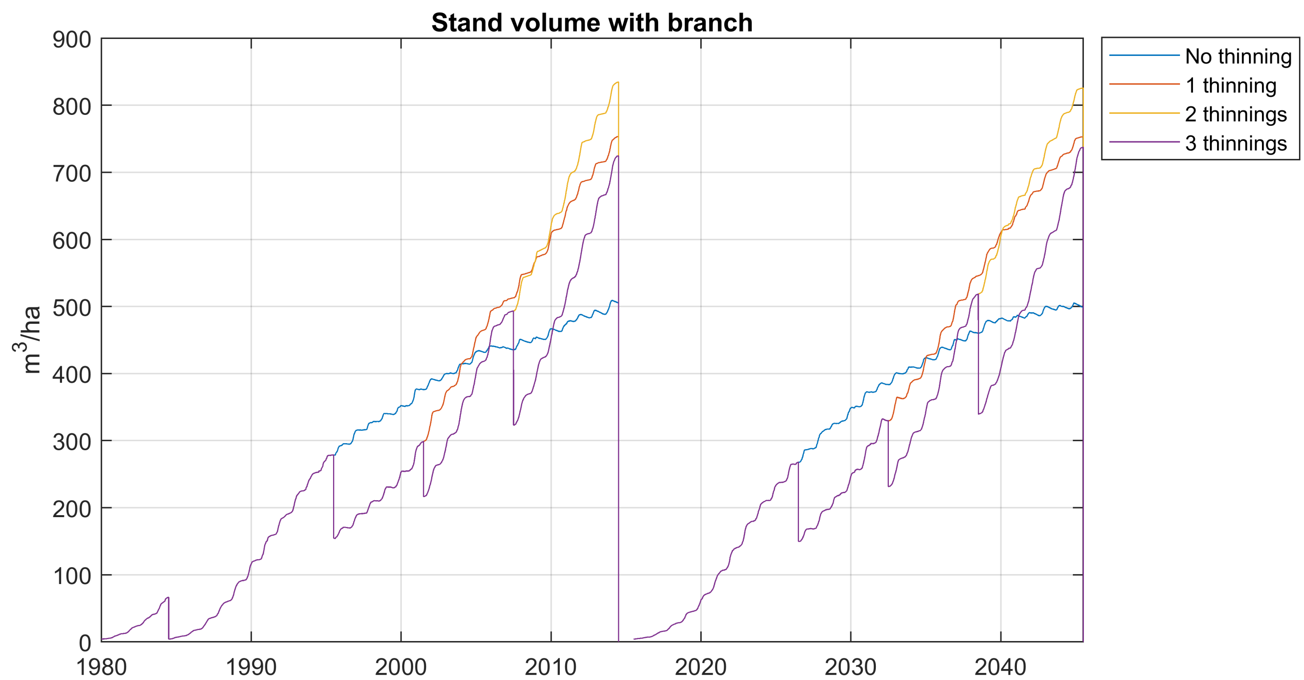

Figure 23. Stand volume with branch (m^3/ha)

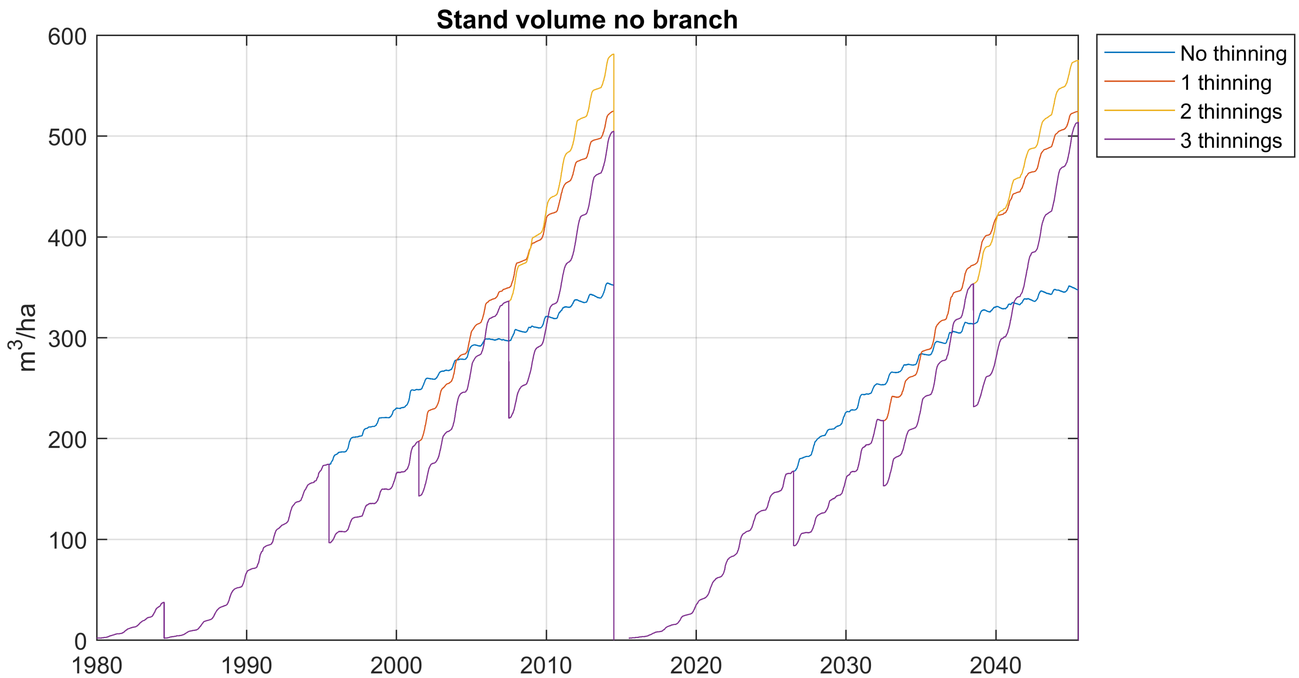

Figure 24. Stand volume no branch (m^3/ha)

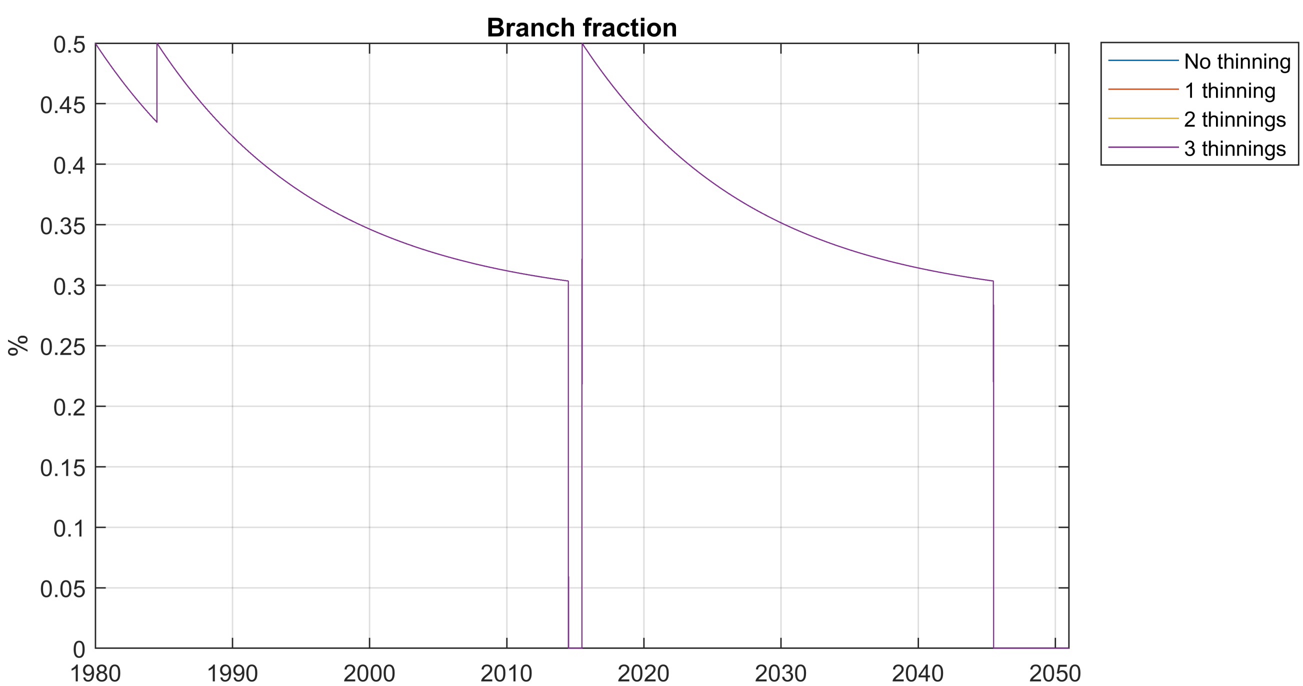

Figure 25. Branch fraction (%)

Soil Water

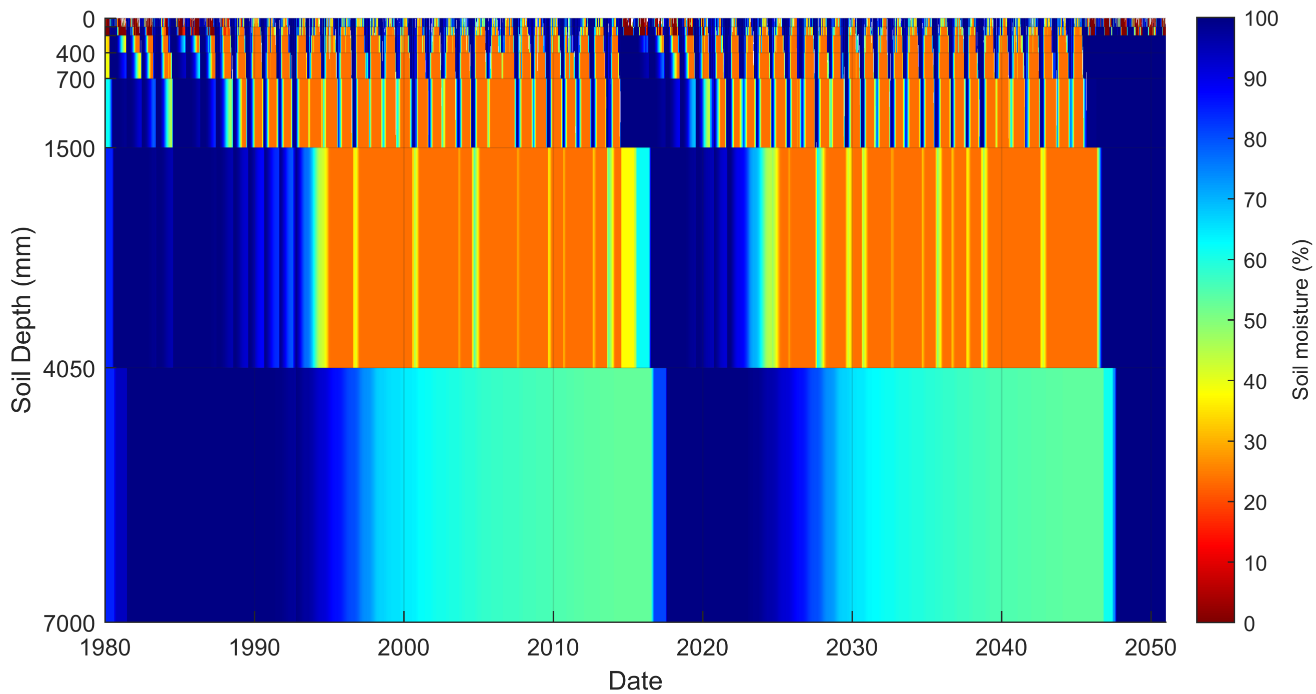

Figure 26. % Soil Moisture: No thinning

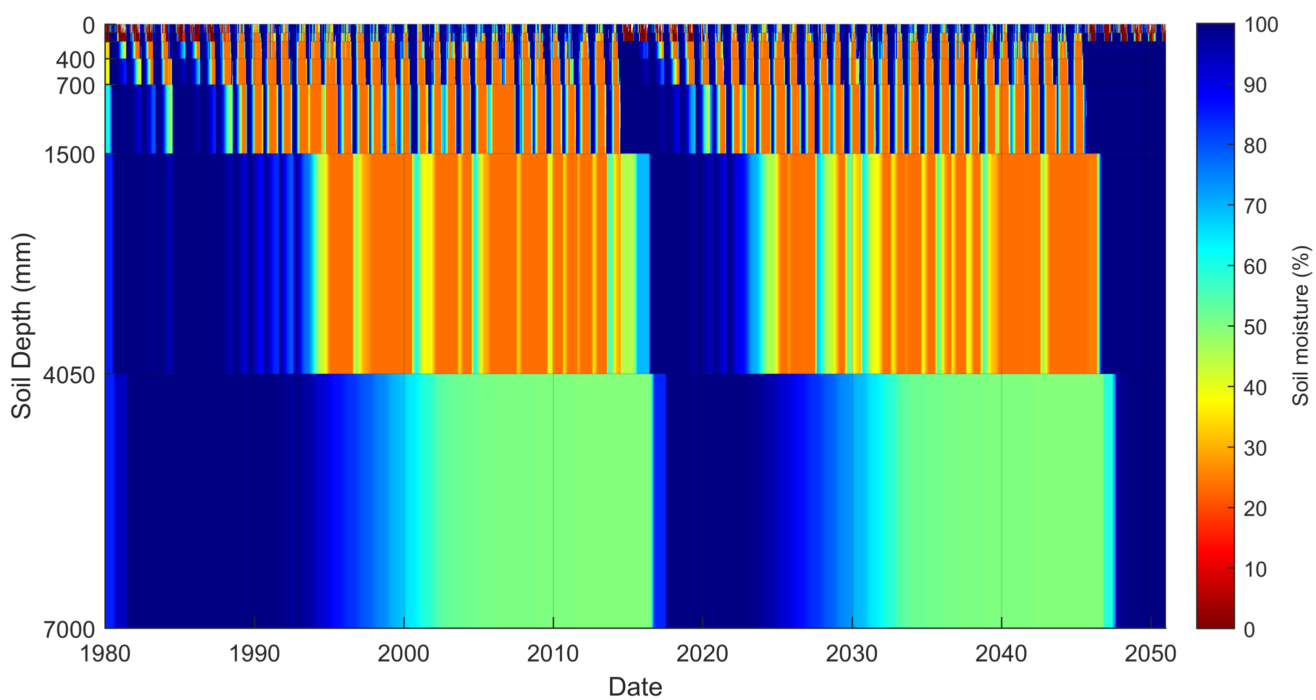

Figure 27. % Soil Moisture: 1 thinning

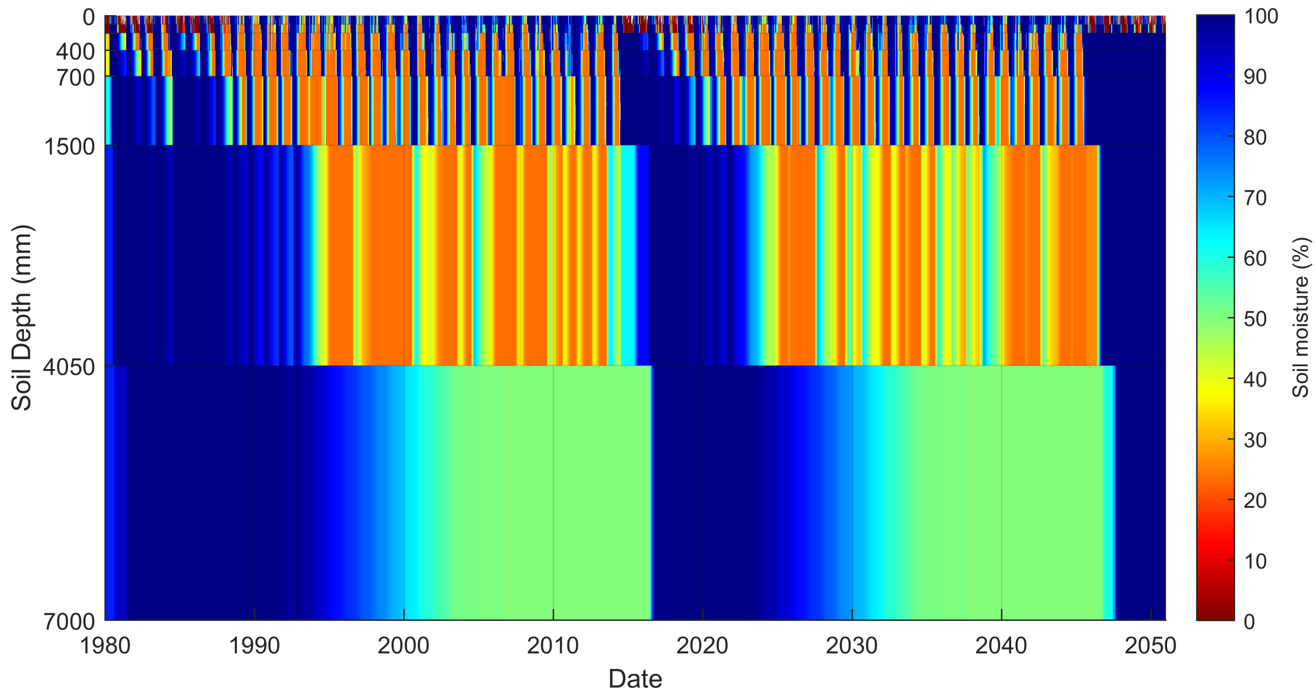

Figure 28. % Soil Moisture: 2 thinnings

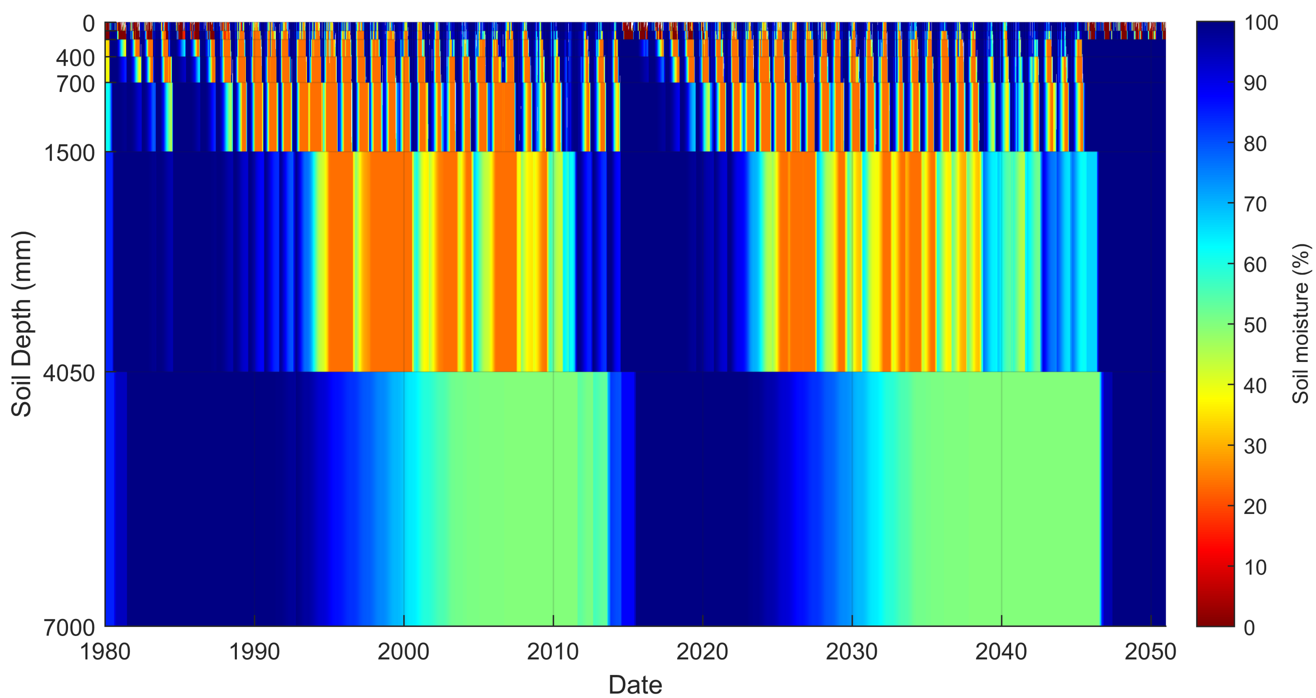

Figure 29. % Soil Moisture: 3 thinnings

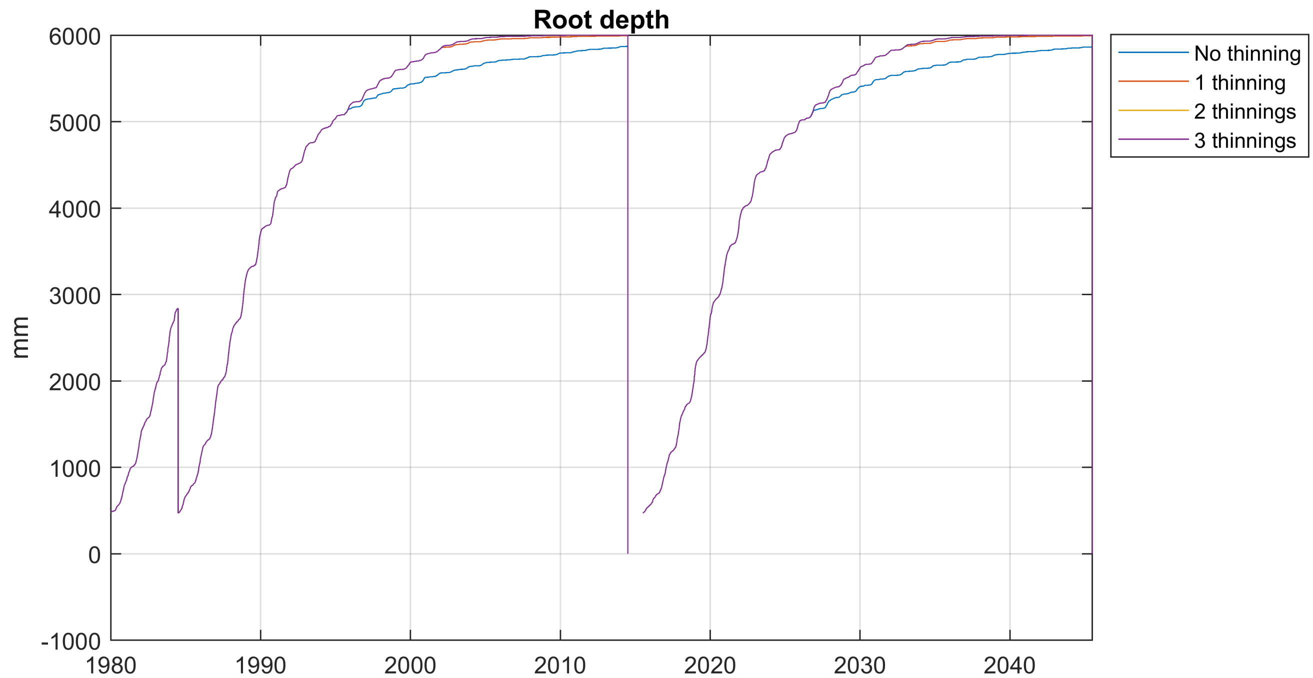

Figure 30. Root depth (mm)

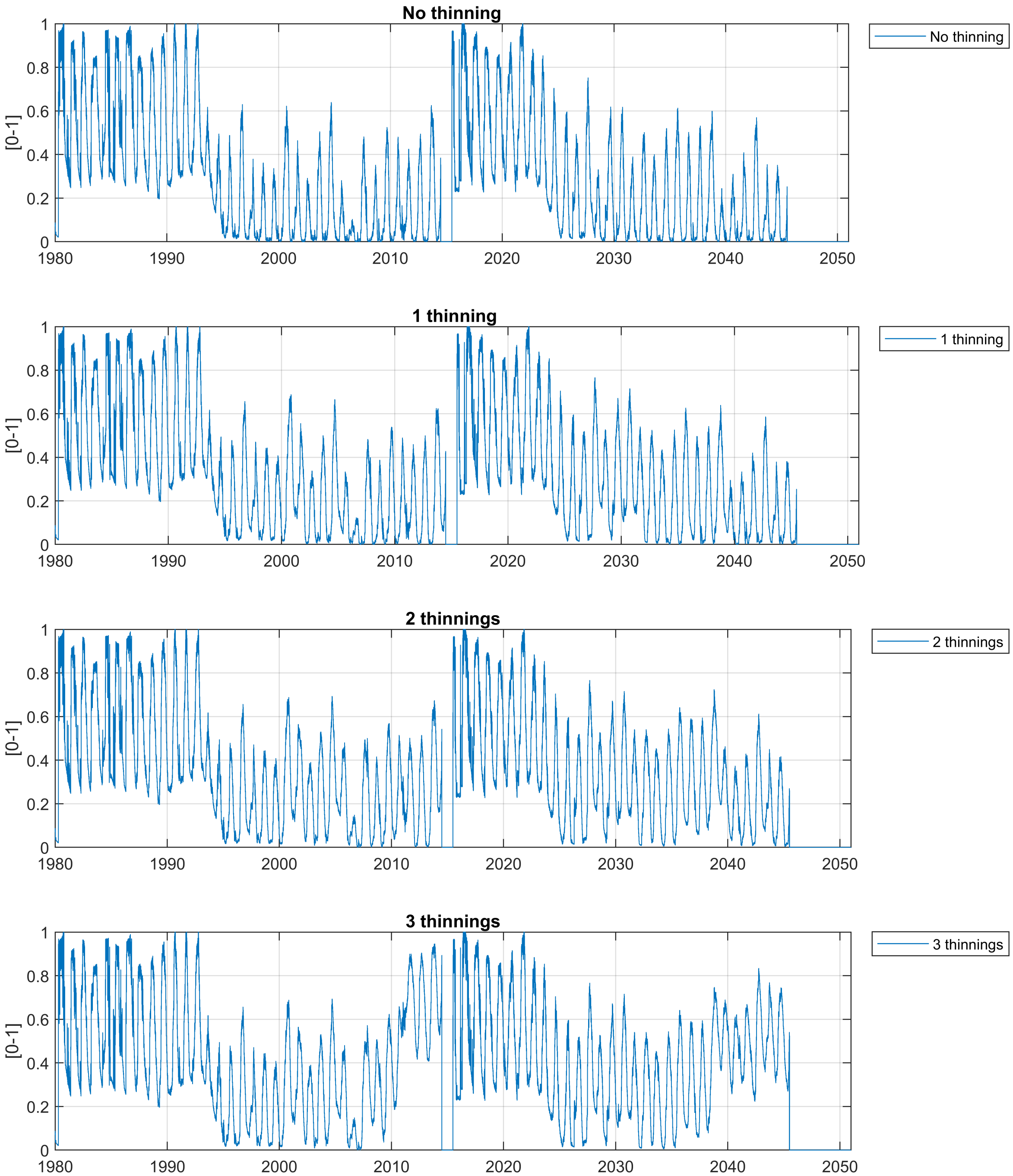
No thinning
No thinning
1 thinning
1 thinning
2 thinnings
2 thinnings
3 thinnings
3 thinnings
[0-1]
0
0.2
0.4
0.6
0.8
1
1980
1990
2000
2010
2020
2030
2040
2050

Figure 31.

References

Allen, R. G., Pereira, L. S., Raes, D., & Smith, M. (1998). FAO Irrigation and drainage paper No. 56. *Rome: Food and Agriculture Organization of the United Nations*, *56*(97), e156.

Beverly, C., 2009. Models of the Catchment Analysis Tool (CAT1D Version 32), August 2009, Technical Reference Manual (ed. C. Beverly), Department of Primary Industries, Victoria.

Beverly, C., Bari, M., Christy, B., Hocking, M., & Smettem, K. (2006). Predicted salinity impacts from land use change: comparison between rapid assessment approaches and a detailed modelling framework. *Australian Journal of Experimental Agriculture*, *45*(11), 1453-1469.

Feikema, P., Morris, J., Beverly, C., Baker, T. and Lane, P. description of the 3PG+ forest growth model. (2010) Department of Forest and Ecosystem Science. The University of Melbourne.

Jeffrey, S.J., Carter, J.O., Moodie, K.B. and Beswick, A.R. (2001). Using spatial interpolation to construct a comprehensive archive of Australian climate data. Environmental Modelling and Software, Vol 16/4, pp 309-330. DOI: 10.1016/S1364-8152(01)00008-1.

Landsberg, J. J., & Waring, R. H. (1997). A generalised model of forest productivity using simplified concepts of radiation-use efficiency, carbon balance and partitioning. *Forest ecology and management*, *95*(3), 209-228.

MATLAB. (2021). version 9.10.0.1602886 (R2021a). Natick, Massachusetts: The MathWorks Inc.

McKenzie, N. J., et al. "Estimation of soil properties using the Atlas of Australian Soils." CSIRO Land and Water Technical Report 11.00 (2000): 1-12.McKenzie, N. J., et al. "Estimation of soil properties using the Atlas of Australian Soils." CSIRO Land and Water Technical Report 11.00 (2000): 1-12.McKenzie, N. J., et al.

Northcote, K.H. and Srene, J.K.M., 1972. Australian soils with saline and sodic properties (No. R&D Rpt).Northcote, K.H. and Srene, J.K.M., 1972. Australian soils with saline and sodic properties (No. R&D Rpt).

Richie, J.T. (1972). A model for predicting evaporation from a row crop with incomplete cover. Water Resources Research, 8, 1204-1213.

Shimano, K. (1997). Analysis of the relationship between DBH and crown projection area using a new model. *Journal of Forest Research*, *2*(4), 237-242.

Weeks A., Beverly C., Whitfield D., and M. Abuzar and J. McInnes (2015). Automated satellite-based estimation of crop water requirement for irrigated horticultural industries in northern Victoria. 21st International Congress on Modelling and Simulation, Gold Coast, Australia, 29 Nov to 4 Dec 2015 www.mssanz.org.au/modsim2015

Weeks, A., Christy, B., Lowell, K., & Beverly, C. (2008). The Catchment Analysis Tool: demonstrating the benefits of interconnected biophysical models. In *Landscape Analysis and Visualisation* (pp. 49-71). Springer, Berlin, Heidelberg.

Weiss, J., Sheffield, K., Weeks, A., & Smith, D. (2019). Modelling the Incursion and Spread of a Forestry Pest: Case Study of Monochamus alternatus Hope (Coleoptera: Cerambycidae) in Victoria. *Forests*, *10*(2), 198.

Appendices

Appendix A

Climate statistics

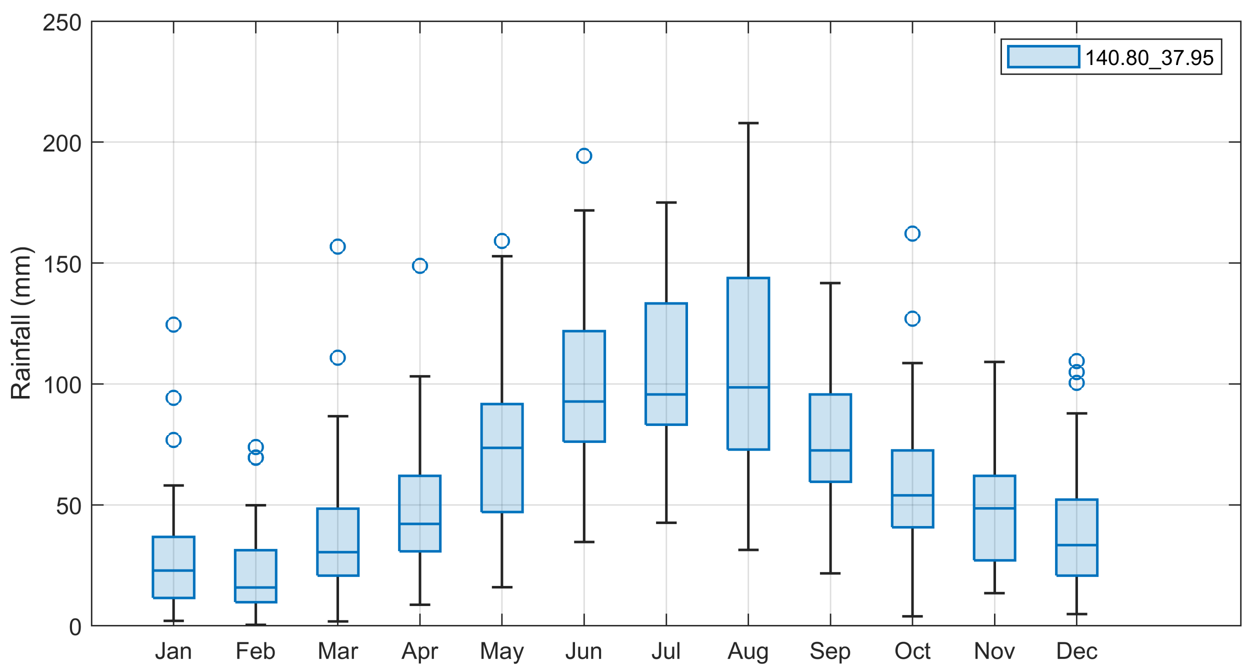

Figure 32. Monthly climate statistics: Rainfall (mm)

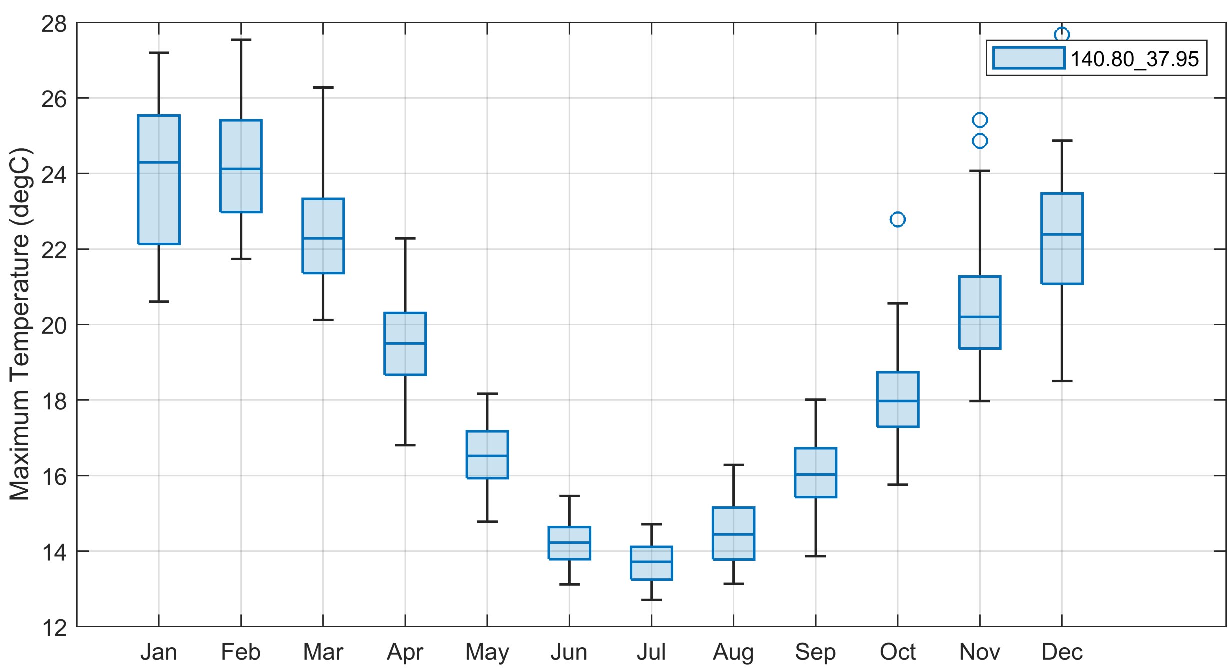

Figure 33. Monthly climate statistics: Maximum Temperature (degC)

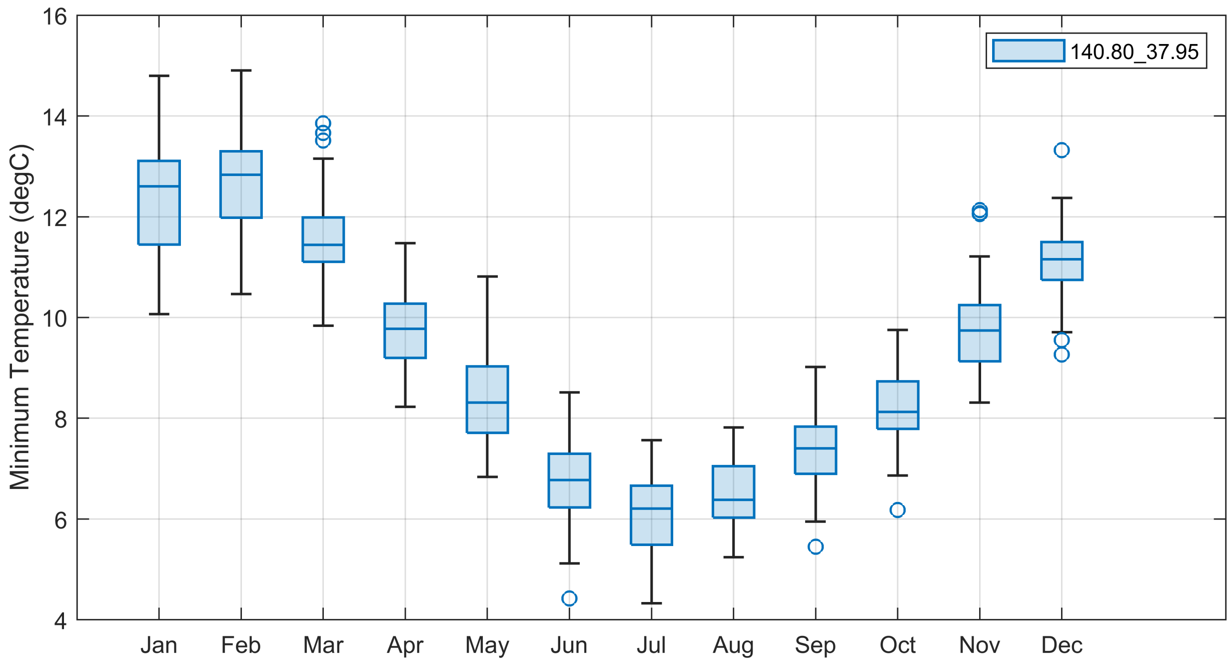

Figure 34. Monthly climate statistics: Minimum Temperature (degC)

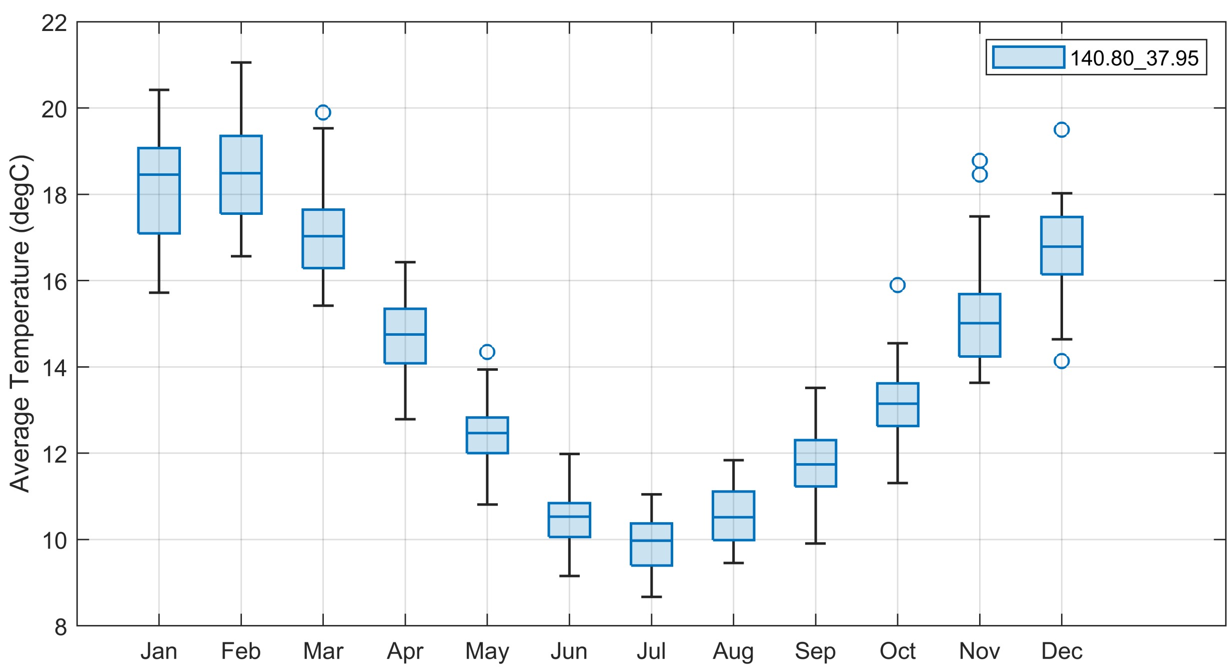

Figure 35. Monthly climate statistics: Average Temperature (degC)

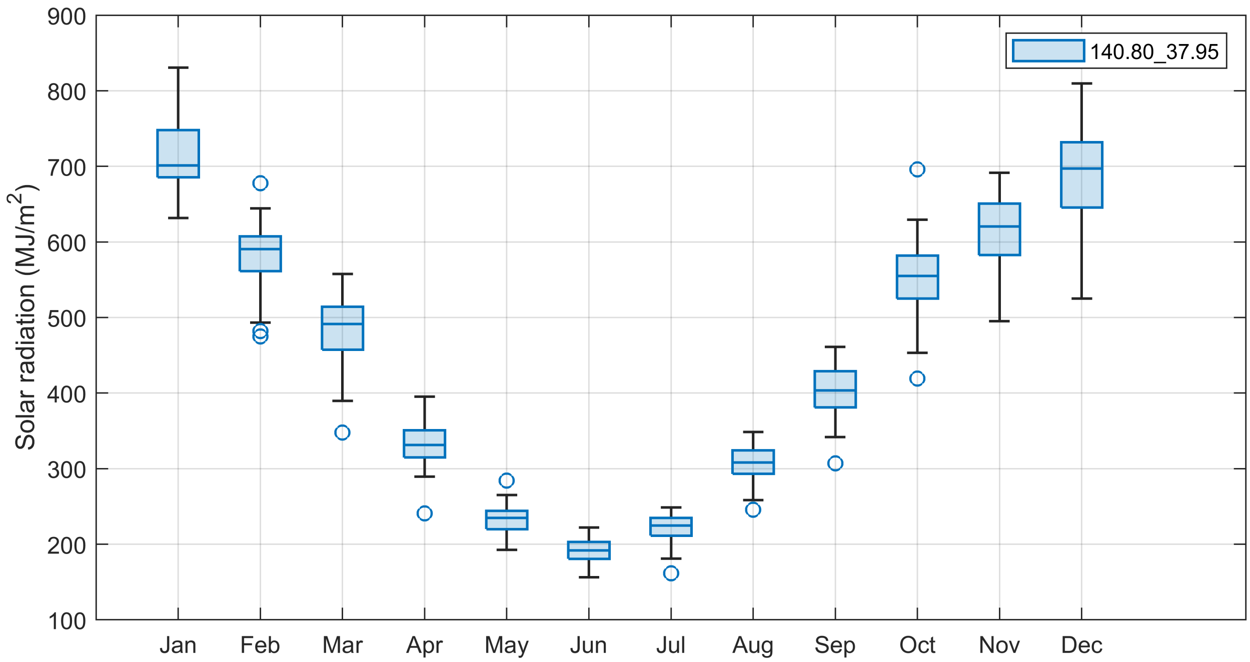

Figure 36. Monthly climate statistics: Solar radiation (MJ/m^2)

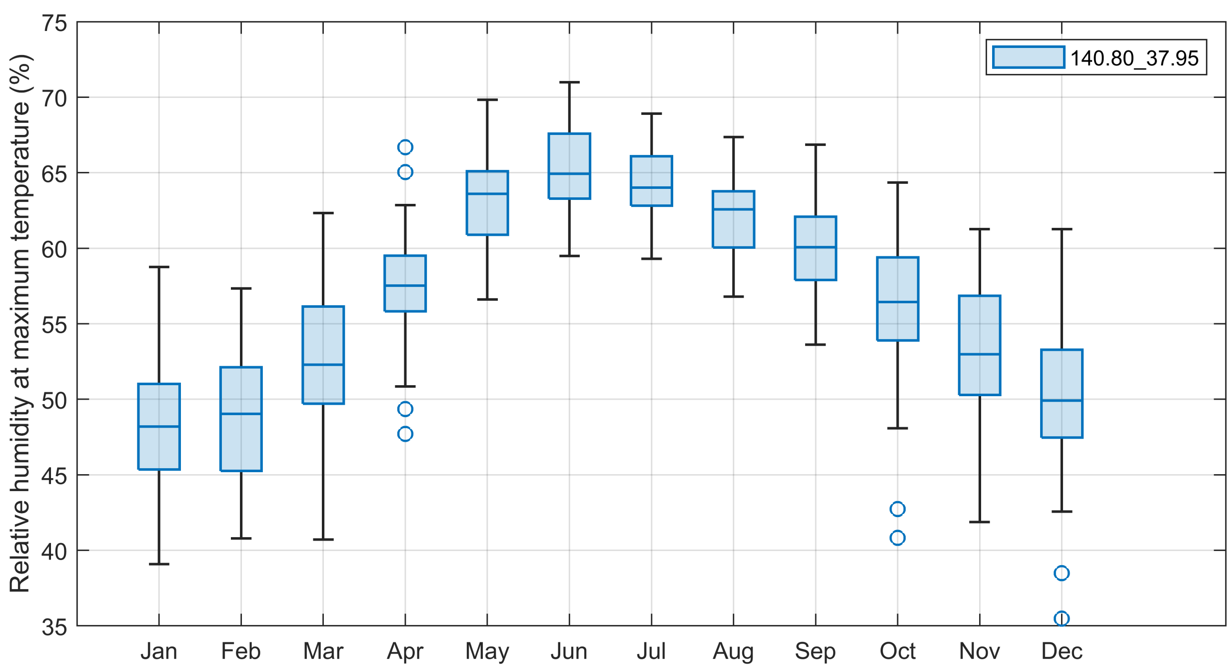

Figure 37. Monthly climate statistics: Relative humidity at maximum temperature (%)

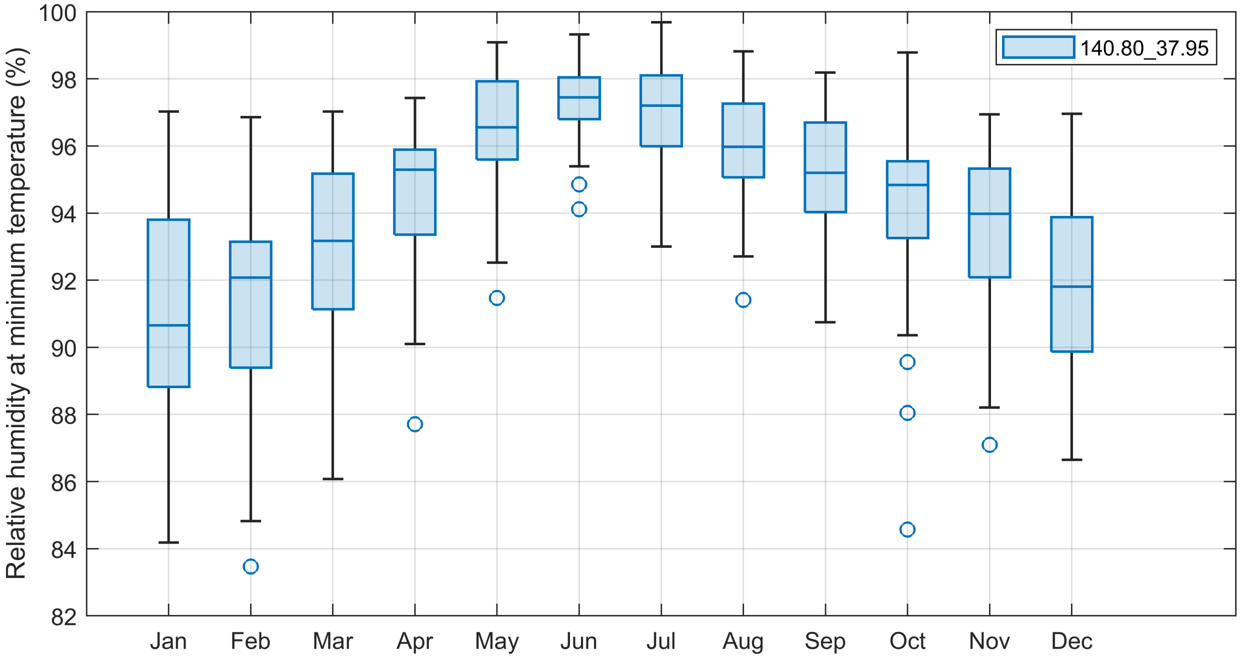

Figure 38. Monthly climate statistics: Relative humidity at minimum temperature (%)

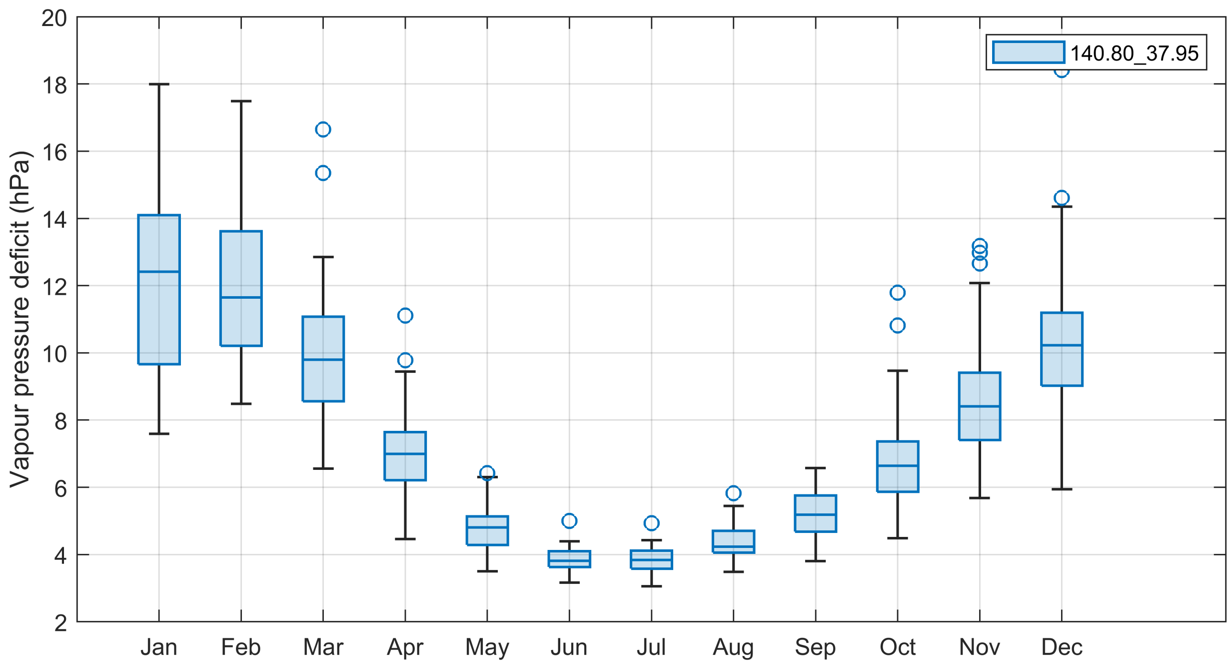

Figure 39. Monthly climate statistics: Vapour pressure deficit (hPa)

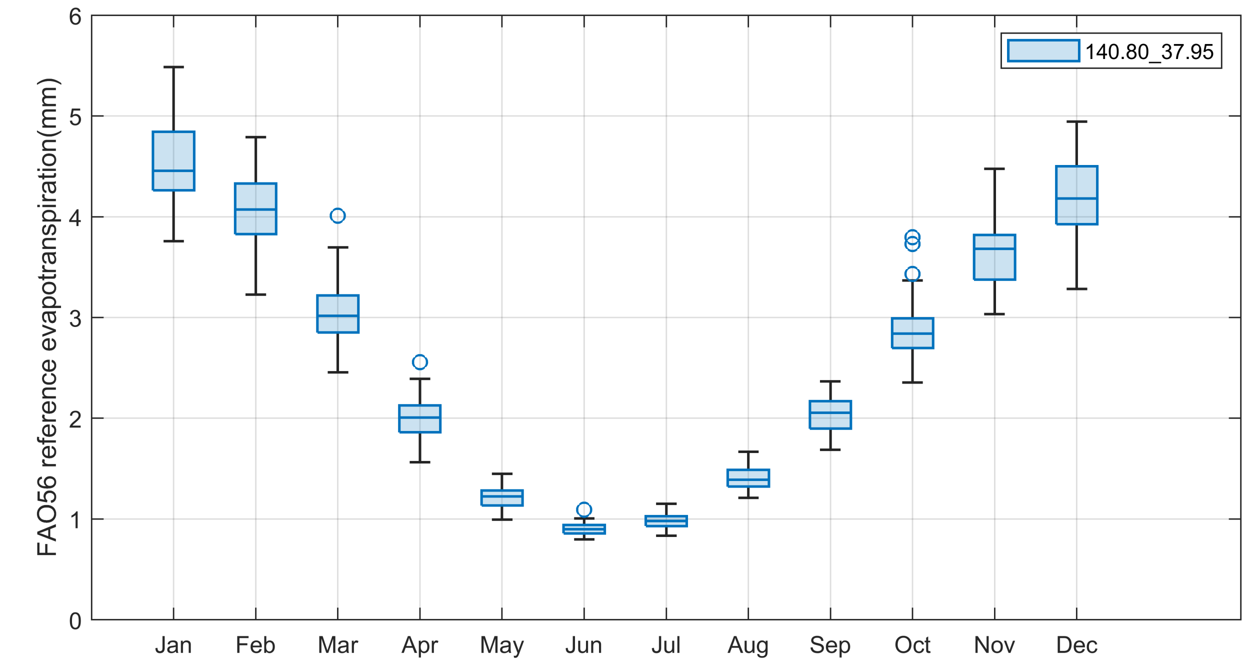

Figure 40. Monthly climate statistics: FAO56 reference evapotranspiration(mm)

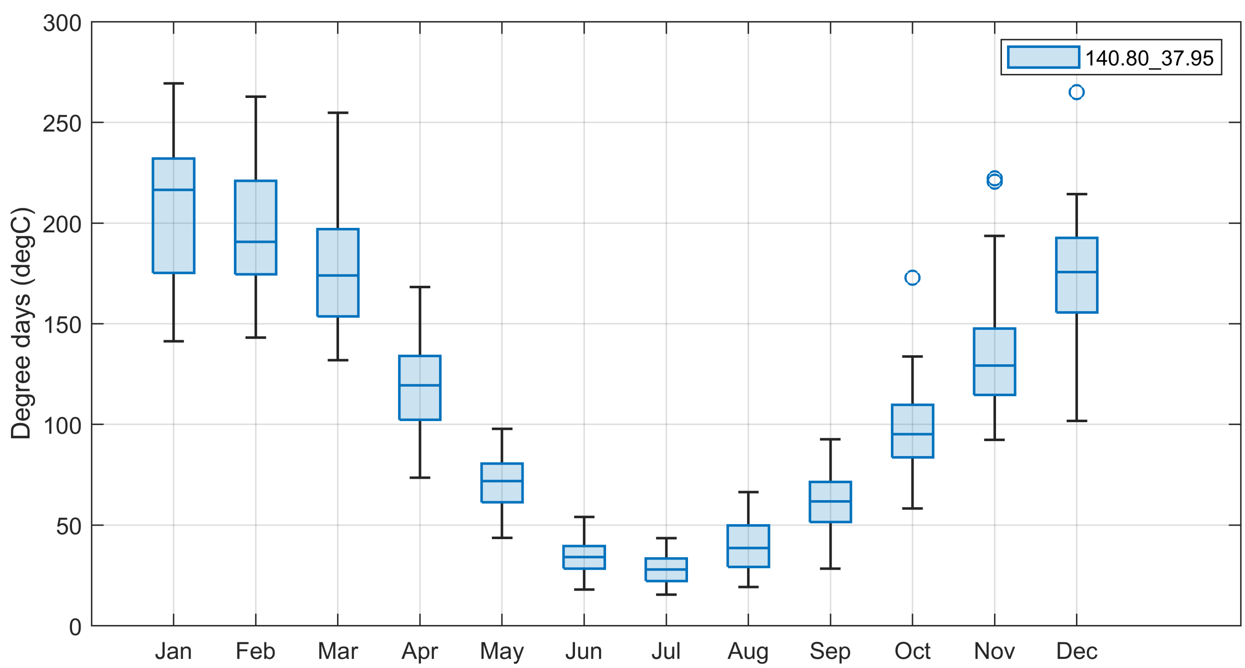

Figure 41. Monthly climate statistics: Degree days (degC)

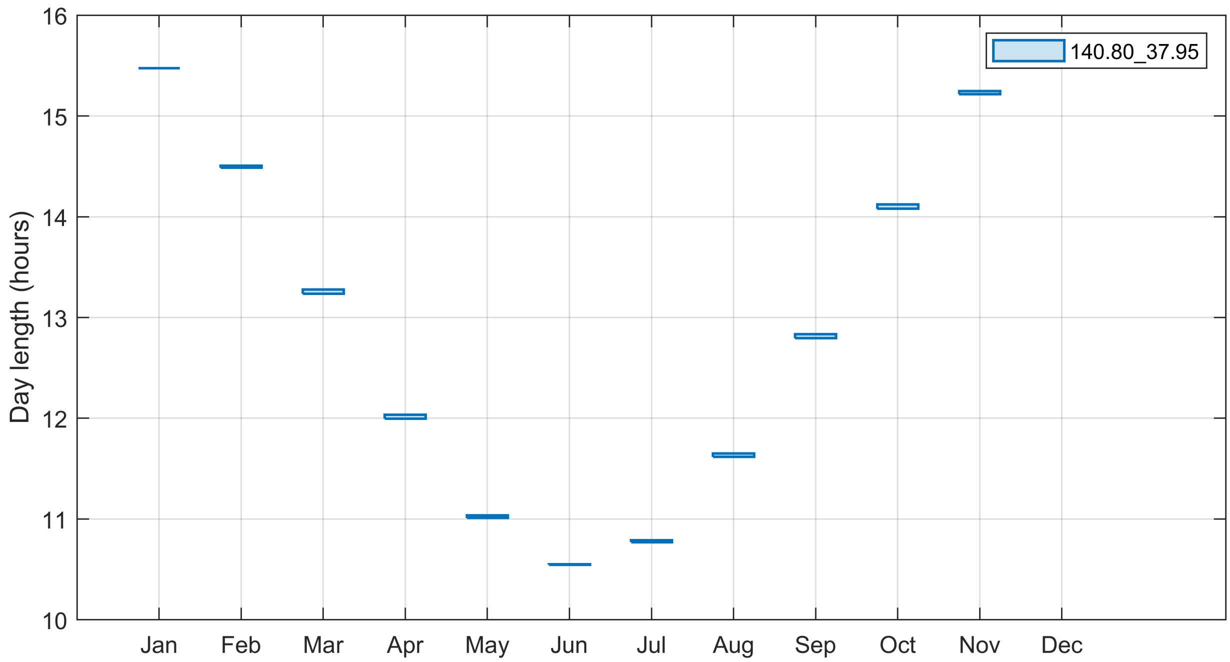

Figure 42. Monthly climate statistics: Day length (hours)

Appendix B

Species parameter sets

Code	Symbol	Pradiata	Description	Units
dwemax	max r_{depth}	6000	Maximum root depth	mm
kphi	k_{ψ}	0.5	Beer's law constant for calculating absorbed radiation	
kg	k_g	0.5	Constant in modifier for canopy conductance (VPD limitation)	
gcmax	g_{cmax}	0.02	Maximum canopy conductance	
maxage	max_{age}	80	Constant for age effect on growth	years
nage	n_{age}	1.8	Power variable for age effect on growth	
alphac	alphaC	1.85	Canopy quantum efficiency	
fertfac	ff	1	Responsiveness of photosynthetic efficiency to nutrition	
cpp	c_{pp}	0.47	Ratio of net to gross primary production	
maintfac	maintfac	0	Maintenance respiration	
initwt	w_{init}	2	Initial mass of a single tree	kg
gammar	γ_r	4.2	Root turnover fraction per month from wrwood to soil	
rootco1	r_a	0.6	Parameter for root allocation	
rootco2	r_b	0.7	Parameter for root allocation	
gammafmax	γ_{fmax}	0.0001	Max. litterfall fraction per month	
cgamma	c_{γ}	5	Constant in litterfall function	
kgamma	k_{γ}	5	Constant in litterfall function	
afco	a_f	0.015	Allometric foliage co-efficient	
nfbase	n_{fbase}	2.3	Allometric foliage co-efficient	
nffac	n_f	0	Allometric foliage co-efficient	
asfac	a_s	0.06	Allometric stem coefficient	
nsfac	n_s	2.7	Allometric stem coefficient	
ctobiomass	$C_{biomass}$	2.2	Factor to convert C mass to biomass DW	kg biomass/kg carbon
denwood	ρ	420	Mean stemwood density	kg/m^3
tmaxpar	T_{max}	32	Maximum temperature for ftemp modifier	ø C
tminpar	T_{min}	5	Minimum temperature for ftemp modifier	ø C
toptpar	T_{opt}	19	Optimum temperature for ftemp modifier	ø C
initbf	BF_{init}	0.5	Branch fraction initial value	
finbf	BF_{final}	0.27	Branch fraction final value	
bfdec	BF_{dec}	-0.08	Branch fraction exponential decline factor	
maxsal	sal_0	15	Salinity in soil water for zero growth	(dS/m) - parts per million (PPM)
initsal	sal_{init}	0	Initial salinity	(dS/m) - parts per million (PPM)
initsla	SLA_{init}	16	Specific Leaf Area of young trees	(m2/kg)
finsla	SLA_{final}	6	Specific Leaf Area of mature trees	(m2/kg)
sladec	SLA_{dec}	-0.4	SLA exponential decline factor	
folfrac	fol_{frac}	0.04	Fraction of initial tree mass that is foliage	
stemfrac	$stem_{frac}$	0.66	Fraction of initial tree mass that is stem	
rootfrac	$root_{frac}$	0.3	Fraction of initial tree mass that is root	
lthresh	l_{thresh}	0.1	Threshold value of ftheta for enhanced litterfall	
littdecay	l_{decay}	0.05	Litter decay rate	
crownfrc	I_1	0.7	Term linking crown storage to LAI	LAI^{-1}
crownppt	I	0.75	Maximum % intercepted rainfall	% rain/day
rd_f	rd_f	0.05	Root extension factor as function of DBH	
maxcrownw	$CrownWidth_{max}$	6.5	Maximum crown width	m
maxcrown_dbh	$DBH_{CrownWidthMax}$	30	DBH at maximum Crown Width	cm
maxrootw	$RootWidth_{max}$	4.5	Maximum horizontal root extension	m